Chapter 9
Turbulence

As we already pinpointed several times in this monograph, turbulent flows occur in many situations in nature and technological applications. It is a subject that started during the nineteenth century and gained much momentum in the last century with the advent of powerful computers enabling solutions of statistical model equations or more recently tackling the full Navier–Stokes equations (without further modeling) through direct numerical simulation (DNS). Turbulence, its understanding and its modeling have been the main concern of many authors, researchers in the physical realm, or in engineering. Without being exhaustive, a few books may be referred to: Batchelor [11], Chassaing [19] (This book is only available in French. It is masterfully written with beautiful figures), Frisch [30], Lesieur [50], McComb [54], Manneville [55], Piquet [73], Pope [74], Tennekes and Lumley [105]. Turbulence modeling is the heart of Chap. 6 of the book by Deville and Gatski [24] where recent methodologies are presented and described in details.

In this chapter we will concentrate our attention to basic topics in turbulent phenomena and set up the standard models used in computational fluid dynamics.

9.1 General Considerations

Turbulence intervenes in most fluid flow phenomena in nature: meteorology, oceanography, hydrography,... or in industrial processes: pipe flows, mixing, melting. The study of turbulent physical phenomena is the main core of intense research, their understanding being not yet complete today.

It is difficult to propose an accurate definition of what is meant by turbulence. However, we can list the general characteristics of turbulent flows:

1. **Unsteadiness**. Turbulent flows are irregular and present a random aspect. A full deterministic approach being impossible, we must resort to statistical methods.
2. **Diffusivity**. The diffusivity of turbulence is the cause of very quick mixings implying momentum and heat transfers.
3. **Dissipative character**. The viscous shear stresses perform a strain work that increases the internal fluid energy at the expense of its turbulent kinetic energy. Turbulence decreases rapidly, if we do not constantly provide energy to the fluid in order to oppose the friction losses, that are more important than in laminar state.
4. **Three-dimensional physics**. Turbulence is rotational and three-dimensional. It is characterized by high levels of vorticity fluctuations. This is the reason why vorticity dynamics plays such an important role.

Turbulence (more specifically developed turbulence) appears for relatively high values of the Reynolds number. It originates in the flow instability generated by the interaction, in the momentum equations, of the viscous and pressure terms and the non-linear terms in the acceleration. This interaction is present only when the inertial effects prevail, i.e. for high values of the Reynolds number. It is understood that turbulence is not an intrinsic characteristics of the fluid, but that it is related to the fluid flow properties.

9.2   General Equations of Incompressible Turbulence

We restrain ourselves in this chapter to the specific case of turbulent incompressible fluid flow. We will write the Navier–Stokes equations in conservative form while neglecting the body forces. Taking the continuity equation into account

$$\operatorname{div} \boldsymbol{v} = \boldsymbol{\nabla} \cdot \boldsymbol{v} = 0 \, , \tag{9.1}$$

the non-linear term reads as a divergence. We have

$$\frac{D\boldsymbol{v}}{Dt} = \frac{\partial \boldsymbol{v}}{\partial t} + (\boldsymbol{\nabla}\boldsymbol{v})\boldsymbol{v} = \frac{\partial \boldsymbol{v}}{\partial t} + \boldsymbol{\nabla} \cdot (\boldsymbol{v} \otimes \boldsymbol{v}) = -\frac{1}{\rho}\boldsymbol{\nabla}\, p + \nu\, \Delta \boldsymbol{v} \, , \tag{9.2}$$

where the symbol $\otimes$ denotes the tensor product of two vectors.

When we examine a velocity signal recorded as a function of time (cf. Fig. 9.1), we are struck by the random character of turbulence. As at each point in space, the velocity and pressure fields offer such temporal variations, we try to drastically reduce the amount of information necessary to interpret the physical phenomena and deduce prediction tools from them for design and engineering purposes. It is illusory to stick to the classical deterministic type modeling which would require following at each point the temporal evolution of velocity and pressure. This would produce a huge database that should be analyzed to extract useful information. Therefore
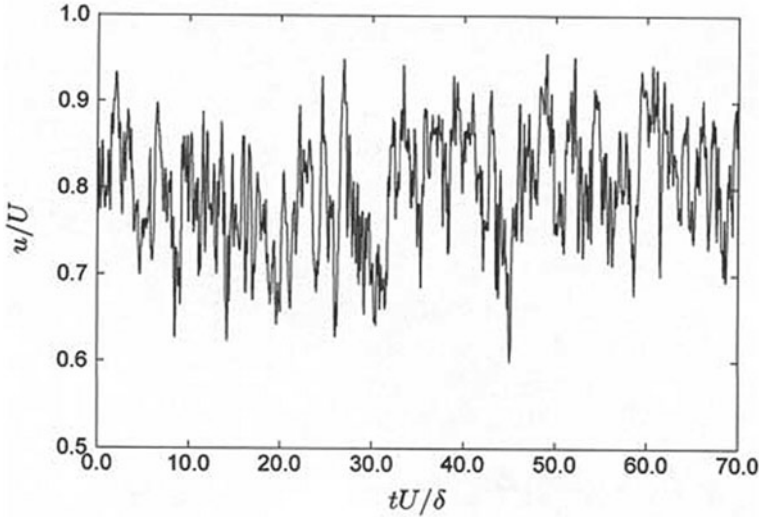
Fig. 9.1 Time variation of instantaneous velocity field at a fixed point within a turbulent boundary layer: $u = v_1$, U mean free-stream velocity and δ boundary layer thickness

the use of a statistical approach is unavoidable. To this end, the velocity vector $\boldsymbol{v}$ is decomposed in an averaged velocity $\overline{\boldsymbol{v}}$ and a fluctuation $\boldsymbol{v}'$ such that

$$\boldsymbol{v} = \overline{\boldsymbol{v}} + \boldsymbol{v}' \ . \tag{9.3}$$

An analogous relation is written for the pressure

$$p = \overline{p} + p' \ . \tag{9.4}$$

This is the Reynolds decomposition of velocity and pressure. The mean velocity $\overline{\boldsymbol{v}}$ is a time average defined by the equation

$$\overline{\boldsymbol{v}} = \lim_{T \to \infty} \frac{1}{T} \int_0^T \boldsymbol{v} \, dt \ . \tag{9.5}$$

This time average cannot be used for flows statistically evolving with time. Furthermore, from the experimental point of view, the measurement time T is such that we continue the averaging process until the moment when the fluctuations of $\overline{\boldsymbol{v}}$ are small enough. If the field is not statistically independent of time, we must take an ensemble average, i.e. the average obtained over a large set of similar experiences

$$< \boldsymbol{v} >= \lim_{N \to \infty} \frac{1}{N} \sum_{n=1}^{N} \boldsymbol{v}_n(\boldsymbol{x}, t) \ . \tag{9.6}$$

We suppose in the sequel that the averaging process is such that the derivatives with respect to space and time commute. The ensemble average satisfies always this property. If the ensemble average defined by (9.6) is an independent quantity of time, then the mean (9.5) is equal to the ensemble average. This is a result of the ergodic theorem, Tennekes and Lumley [105]. (From the statistical point of view, it is equivalent to toss one coin n times and toss n coins once). Note that the average process obtained by (9.6) is linear. However the mean of a product

$$< \boldsymbol{v}_1 \boldsymbol{v}_2 > \tag{9.7}$$

is generally not equal to the product of the means

$$< \boldsymbol{v}_1 >< \boldsymbol{v}_2 > \ .$$

By the definition of the mean, we have the relation

$$\overline{\boldsymbol{v}}' = 0 \ . \tag{9.8}$$

It also follows that given two random functions f and g, one obtains

$$\overline{\overline{f}\,\overline{g}} = \overline{f}\,\overline{g} \tag{9.9}$$

and

$$\overline{\overline{f}\,g'} = 0 \ . \tag{9.10}$$

With the decomposition (9.3), the average of Eq. (9.1) yields

$$\boldsymbol{\nabla} \cdot \overline{\boldsymbol{v}} = 0 \tag{9.11}$$

and therefore,

$$\boldsymbol{\nabla} \cdot \boldsymbol{v}' = 0 \ . \tag{9.12}$$

The fluctuating velocity field is incompressible as is the mean flow.

After inserting (9.3) and (9.4) in (9.2), we compute the mean. The average of the tensor product of the velocities yields

$$\begin{aligned} \overline{\boldsymbol{v} \otimes \boldsymbol{v}} &= \overline{(\overline{\boldsymbol{v}} + \boldsymbol{v}') \otimes (\overline{\boldsymbol{v}} + \boldsymbol{v}')} \\ &= \overline{\overline{\boldsymbol{v}} \otimes \overline{\boldsymbol{v}}} + \overline{\boldsymbol{v}' \otimes \overline{\boldsymbol{v}}} + \overline{\overline{\boldsymbol{v}} \otimes \boldsymbol{v}'} + \overline{\boldsymbol{v}' \otimes \boldsymbol{v}'} \\ &= \overline{\boldsymbol{v}} \otimes \overline{\boldsymbol{v}} + \overline{\boldsymbol{v}' \otimes \boldsymbol{v}'} \ . \end{aligned} \tag{9.13}$$

This procedure generates the Reynolds averaged Navier–Stokes equation (in short RANS)

$$\frac{\partial \overline{\boldsymbol{v}}}{\partial t} + \boldsymbol{\nabla} \cdot (\overline{\boldsymbol{v}} \otimes \overline{\boldsymbol{v}}) = -\frac{1}{\rho} \boldsymbol{\nabla} \overline{p} + \nu \Delta \overline{\boldsymbol{v}} - \boldsymbol{\nabla} \cdot (\overline{\boldsymbol{v}' \otimes \boldsymbol{v}'}) \ . \tag{9.14}$$

Using the average stress tensor defined by the expression

$$\overline{\boldsymbol{\sigma}} = -\overline{p}\,\boldsymbol{I} + 2\,\mu\,\overline{\boldsymbol{d}}\,, \tag{9.15}$$

with tensor $\overline{\boldsymbol{d}}$, the averaged strain rate

$$\overline{\boldsymbol{d}} = \frac{1}{2}(\boldsymbol{\nabla}\overline{\boldsymbol{v}} + (\boldsymbol{\nabla}\overline{\boldsymbol{v}})^{T})\,, \tag{9.16}$$

Equation (9.14) reads

$$\frac{\partial \overline{\boldsymbol{v}}}{\partial t} + \boldsymbol{\nabla}\cdot(\overline{\boldsymbol{v}}\otimes\overline{\boldsymbol{v}}) = \frac{1}{\rho}\boldsymbol{\nabla}\cdot(\overline{\boldsymbol{\sigma}} - \rho\overline{\boldsymbol{v}'\otimes\boldsymbol{v}'})\,. \tag{9.17}$$

By similarity with the average Cauchy tensor $\overline{\boldsymbol{\sigma}}$, the second term under the operator $\boldsymbol{\nabla}\cdot$ is assimilated to a stress, known as the symmetric Reynolds stress tensor $\boldsymbol{R}$

$$\boldsymbol{R} = -\rho\,\boldsymbol{\tau} = -\rho\overline{\boldsymbol{v}'\otimes\boldsymbol{v}'}\,, \tag{9.18}$$

while $\boldsymbol{\tau}$ has dimensions of squared velocities. This tensor will be named Reynolds tensor with no reference to stress. Note that $\boldsymbol{\tau}$ is similar to an energy tensor.

Equations (9.11) and (9.14) form a system of four equations with 10 unknowns, namely the three velocity components $\overline{v}_i$, the pressure $\overline{p}$ and the six components τ_{ij}. The Eqs. (9.17) and (9.18) exhibit the coupling between the average field and the fluctuation. We observe also that with more unknowns than equations, the closure problem is posed.

Subtracting the mean momentum equation (9.14) from the Navier–Stokes equation (9.2) gives the momentum equation of the fluctuating field that highlights the coupling with the mean field

$$\frac{\partial \boldsymbol{v}'}{\partial t} + \boldsymbol{\nabla}\cdot(\boldsymbol{v}'\otimes\overline{\boldsymbol{v}}) = -\boldsymbol{\nabla}\cdot(\overline{\boldsymbol{v}}\otimes\boldsymbol{v}') - \boldsymbol{\nabla}\cdot(\boldsymbol{v}'\otimes\boldsymbol{v}' - \overline{\boldsymbol{v}'\otimes\boldsymbol{v}'}) - \frac{1}{\rho}\boldsymbol{\nabla}p' + \nu\Delta\boldsymbol{v}'\,. \tag{9.19}$$

9.3 Kinetic Energy

Let us define the turbulent kinetic energy of the fluctuations, K, by the relation

$$K = \frac{1}{2}\overline{\boldsymbol{v}'\cdot\boldsymbol{v}'}\,. \tag{9.20}$$

This turbulent energy may be obtained as the half-trace of tensor $\boldsymbol{\tau}$

$$K = \frac{1}{2}\tau_{ii} \; . \tag{9.21}$$

The momentum equation of the turbulent kinetic energy is gotten by multiplying Eq. (9.19) by $\boldsymbol{v}'$ and taking the mean. We have

$$\frac{\partial K}{\partial t} + \overline{\boldsymbol{v}} \cdot \nabla K = -\boldsymbol{\tau} : \nabla \overline{\boldsymbol{v}} - \nu\overline{\nabla \boldsymbol{v}' : \nabla \boldsymbol{v}'} - \nabla \cdot \boldsymbol{j} \; , \tag{9.22}$$

where the flux vector of turbulent kinetic energy $\boldsymbol{j}$ is defined by

$$\boldsymbol{j} = \frac{1}{\rho}\overline{p'\boldsymbol{v}'} + \frac{1}{2}\overline{(\boldsymbol{v}' \cdot \boldsymbol{v}')\boldsymbol{v}'} - \nu\nabla K \; . \tag{9.23}$$

We notice in (9.23) the appearance of the triple velocity correlation. The first and second terms of the right hand side of (9.22) are the production rates of turbulent energy $\mathcal{P}$ and of dissipation of turbulent energy $\mathcal{D}$, respectively. We will denote them

$$\mathcal{P} = -\boldsymbol{\tau} : \nabla \overline{\boldsymbol{v}} = -\boldsymbol{\tau} : \overline{\boldsymbol{d}}, \tag{9.24}$$
$$\mathcal{D} = \nu\overline{\nabla \boldsymbol{v}' : \nabla \boldsymbol{v}'} \; . \tag{9.25}$$

The production $\mathcal{P}$ is the result of the inner product of Reynolds tensor and the mean strain rate tensor. We observe that it is most often positive, although there might be situations where it is negative.

As the source of turbulent kinetic energy is the mean flow, we should retrieve this term with its sign changed in the equation governing the average kinetic energy, E_k, defined by the relation

$$E_k = \frac{1}{2}\overline{\boldsymbol{v}} \cdot \overline{\boldsymbol{v}} \; . \tag{9.26}$$

Let us multiply Eq. (9.14) by $\overline{\boldsymbol{v}}$. After some tedious but simple manipulations, one obtains:

$$\frac{\partial E_k}{\partial t} + \overline{\boldsymbol{v}} \cdot \nabla E_k = -\frac{1}{\rho}\nabla \cdot (\overline{p}\,\overline{\boldsymbol{v}}) - 2\nu\,\overline{\boldsymbol{d}} : \overline{\boldsymbol{d}} + 2\nu\,\nabla \cdot (\overline{\boldsymbol{v}}\,\overline{\boldsymbol{d}}) - \mathcal{P} - \nabla \cdot (\overline{\boldsymbol{v}}\,\boldsymbol{\tau}) \; . \tag{9.27}$$

In (9.27), appears the right product of tensor $\overline{\boldsymbol{d}}$ and the vector $\overline{\boldsymbol{v}}$. In indexed form, this product reads

$$(\overline{\boldsymbol{v}}\,\overline{\boldsymbol{d}})_j = \overline{v}_i\overline{d}_{ij} \; . \tag{9.28}$$

In the right hand side of (9.27), we find successively the following terms. The first one is associated with pressure and expresses the flow power. The two terms involving viscosity are one, the dissipation rate of turbulent kinetic energy by the molecular

viscous effects and the other, a reversible transfer of viscous power. The fourth term is a sink of mean turbulent kinetic energy $-\mathcal{P}$. Finally the last term is a divergence. If it is integrated on a sufficiently large volume, bounded by fluid in laminar flow, this term vanishes. Thus it takes into account a conservative transfer in the volume of mean kinetic energy.

9.4 Dynamic Equation of the Reynolds Tensor

This equation is developed by multiplying the momentum equation (9.19) of fluctuation v_i' by v_j' and the one of fluctuation v_j' by v_i'. Adding the resulting equations and averaging, one obtains

$$\frac{\partial \boldsymbol{\tau}}{\partial t} + \overline{\boldsymbol{v}} \cdot \nabla \boldsymbol{\tau} = \boldsymbol{P} + \boldsymbol{\Pi} - \boldsymbol{D} - \nabla \cdot \boldsymbol{J}^{(3)} . \tag{9.29}$$

Recall that the inner product of two tensors $\boldsymbol{A}$ and $\boldsymbol{B}$ is written in indexed notation as $(\boldsymbol{AB})_{ij} = A_{im} B_{mj}$; thus, $(\boldsymbol{AB}^T)_{ij} = A_{im} B_{jm}$. Consequently the production term

$$\boldsymbol{P} = -(\boldsymbol{\tau}\, (\nabla \overline{\boldsymbol{v}})^T + (\nabla \overline{\boldsymbol{v}})\, \boldsymbol{\tau}^T) \tag{9.30}$$

is the source of the Reynolds stresses. We note that its trace yields

$$tr\, \boldsymbol{P} = 2\mathcal{P} . \tag{9.31}$$

The correlation term of pressure-strain rate

$$\boldsymbol{\Pi} = \frac{1}{\rho}\, \overline{p'(\nabla \boldsymbol{v}' + (\nabla \boldsymbol{v}')^T)} \tag{9.32}$$

possesses a zero trace. It redistributes the energy among the components of normal stresses as it contributes to an exchange between the components $\overline{v_1'^2}, \overline{v_2'^2}, \overline{v_3'^2}$ without modifying their sum. The dissipation-rate term

$$\boldsymbol{D} = 2\nu\, \overline{(\nabla \boldsymbol{v}')(\nabla \boldsymbol{v}')^T} \tag{9.33}$$

has a trace whose value is

$$tr\, \boldsymbol{D} = 2\,\mathcal{D} . \tag{9.34}$$

Finally the tensor of order three, $\boldsymbol{J}^{(3)}$, is given by the equation

$$\boldsymbol{J}^{(3)} = \frac{1}{\rho}\, (\overline{p' \boldsymbol{v}'} \boldsymbol{I} + (\overline{p' \boldsymbol{v}'} \boldsymbol{I})^T) + \overline{\boldsymbol{v}' \otimes \boldsymbol{v}' \otimes \boldsymbol{v}'} - \nu \nabla \boldsymbol{\tau} . \tag{9.35}$$

The first term is the exterior product of vector $\overline{p'\boldsymbol{v'}}$ and the identity tensor $\boldsymbol{I}$

$$(\overline{p'\boldsymbol{v'}\boldsymbol{I}})_{ijk} = \overline{p'v'_i}\,\delta_{jk}\ . \tag{9.36}$$

The second term is the transpose, the last index remaining unchanged, such that

$$(\overline{p'\boldsymbol{v'}\boldsymbol{I}})_{ijk}^T = \overline{p'v'_j}\delta_{ik}\ . \tag{9.37}$$

The third term $\overline{\boldsymbol{v'}\otimes\boldsymbol{v'}\otimes\boldsymbol{v'}}$ is the triple velocity correlation defined by the tensor product of three vectors, namely

$$(\overline{\boldsymbol{v'}\otimes\boldsymbol{v'}\otimes\boldsymbol{v'}})_{ijk} = \overline{v'_i v'_j v'_k}\ . \tag{9.38}$$

Finally the gradient of the second order tensor $\boldsymbol{\tau}$ is a third-order tensor with components

$$(\boldsymbol{\nabla\tau})_{ijk} = \frac{\partial}{\partial x_k}\tau_{ij}\ . \tag{9.39}$$

The tensor $\boldsymbol{J}^{(3)}$ is diffusive in essence and induces a spatial redistribution of energy (cf. the divergence theorem). We notice that in Eq. (9.29), the non-linear terms have generated triple velocity correlations $\overline{v'_i v'_j v'_k}$. It is possible to write the dynamic equations that govern the evolution of these triple correlations; they will call for quadruple correlations. The dynamics of quadruple correlations will entail quintuple correlations, and so forth. The mathematical complications will increase at each step. The hierarchy of the equations for the moments (averages of higher order products of velocity fluctuations) is not only infinite but also divergent, in the sense that additional unknowns produced at each stage appear in greater number than that of new equations. To overcome this difficulty, the problem is simplified in order to close the open equations hierarchy. This procedure is called the closure problem.

The simplest closure consists in truncating the set of equations with the assumption that the correlations are negligible beyond a certain order, in practice, the third or fourth order. We try then to express the high order correlations in terms of smaller order correlations.

A classification of turbulence models is based on the number of additional partial differential equations (with respect to the average Navier–Stokes equations) required to close the model.

The zero equation model consists in retaining only order two moments and therefore in linking the turbulent stress tensor to some characteristics of the mean flow via a turbulent viscosity. The one equation model, also called K model, is due to Prandtl. A partial differential equation is used to describe the dynamics of the turbulent kinetic energy. Eventually the two equation model is based on the dynamics of the turbulent kinetic energy and its dissipation rate. It is the well known $K - \varepsilon$ model.

9.5   Structures and Scales of Homogeneous Turbulence

Turbulence is homogeneous when the averaged quantities are invariant by spatial translation. Particularly, the mean velocity field in homogeneous turbulence is independent of the position x. We then conclude that in homogeneous turbulence, all spatial points are statistically equivalent. If moreover, these statistical properties are independent of the orientation of the frame of reference, the field is called isotropic. The homogeneous and isotropic turbulence (HIT) allows using Fourier methods to build analytical turbulence models.

Experimentally and theoretically, it is observed that turbulence dynamics is strongly linked to vorticity dynamics. The vorticity filaments are stretched and twisted. This phenomenon is at the origin of the creation of large vorticity structures (large eddies). The large scales are very efficient to generate the Reynolds stresses that extract their energy from the mean flow. Through non-linear interactions, that are inviscid processes, the turbulent energy is transferred to smaller and smaller sized vortices. The viscosity only comes into play for sufficiently small vortices, of the order of Kolmogorov scale defined later, where this energy is dissipated.
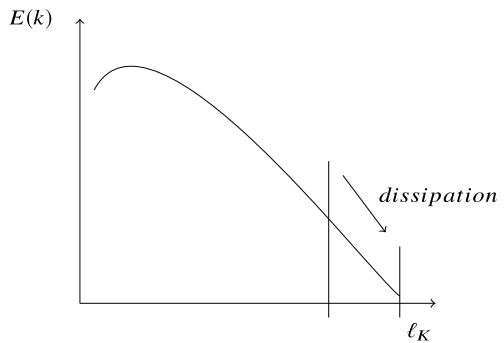
Experiments lead to assuming the existence of an energy transfer from the large scales to the small ones without any dissipation. This is viewed as the energy cascade (or Richardson's cascade). Let us note that locally, "inverse" fluxes exist and give rise to the formation of larger scales from smaller ones. This is called retro-diffusion. Figure 9.2 shows the spectral energy $E(k)$ (introduced in the sequel) as a function of the Kolmogorov scale ℓ_K. Dissipation occurs for the small scale structures.

We will suppose that dissipation characterized by its dissipation rate ε ($\mathrm{m^2\,s^{-1}}$) operating at the level of small vortices arises from the large scales and that the turbulent energy is linked to them. Therefore if one chooses K and ε to qualify these large structures, by dimensional analysis, we obtain for their characteristic length

$$\ell = K^{3/2}/\varepsilon \qquad\qquad (9.40)$$

with ε defined by the relation

Fig. 9.2   Energy cascade

$$\varepsilon = 2\nu \overline{\boldsymbol{d'} : \boldsymbol{d'}} = \nu \overline{\frac{\partial v_i'}{\partial x_j}\left(\frac{\partial v_i'}{\partial x_j} + \frac{\partial v_j'}{\partial x_i}\right)} = \frac{\nu}{2}\overline{\left(\frac{\partial v_i'}{\partial x_j} + \frac{\partial v_j'}{\partial x_i}\right)^2} .$$
(9.41)

The characteristic time scale of these large vortices is given by

$$\tau = K/\varepsilon$$
(9.42)

with $K^{1/2}$ as the velocity scale. The turbulence Reynolds number rests upon the previous scales and reads

$$Re_T = \frac{K^{1/2}\ell}{\nu} = \frac{K^2}{\varepsilon \nu} .$$
(9.43)

Very often, the turbulence Reynolds number is smaller than the physical Reynolds number of the flow by a factor in between 20 and 100. The scale ℓ (9.40) of vortices energetic enough to influence the mean momentum is called mixing length. At the other end of the energy cascade, we find small vortices that are determined essentially by ε and ν. Dimensional analysis yields the Kolmogorov scale ℓ_K defined by the relationship

$$\ell_K = (\nu^3/\varepsilon)^{1/4}$$
(9.44)

corresponding to the scale where dissipative viscous phenomena start acting on the vortices that have a size of the order of that scale, and time τ_K

$$\tau_K = (\nu/\varepsilon)^{1/2}$$
(9.45)

characterizing the lifetime of a vortex of size $\sim \ell_K$. As we can admit that viscosity will fully play its role if the Reynolds number associated to small structures are of the order of unity, we can set that

$$\frac{v_K \ell_K}{\nu} \approx 1 .$$
(9.46)

Thus we obtain

$$v_K = (\nu\varepsilon)^{1/4} .$$
(9.47)

Dividing (9.40) by (9.44), the ratio of large to small scales constitute an estimate of the spectrum:

$$\frac{\ell}{\ell_K} = Re_T^{3/4} .$$
(9.48)

With (9.48), when the Reynolds number increases, it is the chain of space structures that spreads (often over several decades). This large range limits the direct numerical simulations to low or moderate Reynolds numbers. On the contrary, the large eddy simulation where the structures of smaller size than the mesh step are modeled, depends precisely on these models. It is considered that small scale turbulence is

homogeneous and that small scales dynamics is isotropic, and consequently more universal than that of the large scales. Thus, it is necessary to understand what is meant by HIT.

9.6 Homogeneous Turbulence

Homogeneous turbulence is described within the framework of the statistical properties of random homogeneous fields. To this end, we need to introduce the concept of correlations and spectra. In this section we follow closely the presentation of the subject by W. C. Reynolds [78].

9.6.1 Correlations and Spectra

Let f and g denote two random fields. Then the two-point correlation of f and g is defined by the relation

$$Q_{fg}(\boldsymbol{x}, \boldsymbol{x}', t) = \langle \overline{f(\boldsymbol{x}, t)g(\boldsymbol{x}', t)} \rangle \qquad (9.49)$$

with upper line for the volume average

$$\overline{f}(t) = \lim_{L \to \infty} \frac{1}{L^3} \int_0^L f(\boldsymbol{x}, t)\, d^3\boldsymbol{x} \qquad (9.50)$$

and the brackets for the ensemble mean. For homogeneous fields, the ergodic assumption implies the equivalence of these two types of averaging.

For homogeneous fields, Q_{fg} depends only on the distance between the two points $\boldsymbol{r} = \boldsymbol{x}' - \boldsymbol{x}$ and on t

$$Q_{fg}(\boldsymbol{r}, t) = \langle \overline{f(\boldsymbol{x}, t)g(\boldsymbol{x} + \boldsymbol{r}, t)} \rangle. \qquad (9.51)$$

In homogeneous turbulence, we use Fourier series to represent the fields, with the hypothesis that turbulence occurs in a cube with a periodicity of length L. Most of the time, for the sake of simplicity and ease of analysis, one chooses $L = 2\pi$. This procedure allows to forget about the influence of the boundary conditions on the flow and to rely on the space periodicity of the fields.

The representation of $f(\boldsymbol{x})$ reads

$$f(\boldsymbol{x}) = \sum_{\boldsymbol{k}} \hat{f}(\boldsymbol{k})\, e^{-i\boldsymbol{k}\cdot\boldsymbol{x}}, \quad -\infty < k < +\infty, \qquad (9.52)$$

where $\hat{f}(\boldsymbol{k})$ is the associated spectrum to f. The three-dimensional wave-vector $\boldsymbol{k}$ is such that $\boldsymbol{k} = (k_1, k_2, k_3)$. Imposing that $f(\boldsymbol{x})$ be a real function implies

$$\hat{f}(\boldsymbol{k}) = \hat{f}^*(-\boldsymbol{k}) \tag{9.53}$$

with the symbol $*$ denoting the conjugate complex. The relation (9.53) is the Hermitian property.

   To express the two point correlation between f and g, we write

$$\langle f(\boldsymbol{x})g(\boldsymbol{x}')\rangle = \sum_{\boldsymbol{k}}\sum_{\boldsymbol{k}'}\langle \hat{f}(\boldsymbol{k})\hat{g}(\boldsymbol{k}')\rangle e^{-i(\boldsymbol{k}\cdot\boldsymbol{x}+\boldsymbol{k}'\cdot\boldsymbol{x}')} \ . \tag{9.54}$$

Setting $\boldsymbol{k}'' = -\boldsymbol{k}'$ and $\boldsymbol{r} = \boldsymbol{x}' - \boldsymbol{x}$, we get

$$\langle f(\boldsymbol{x})g(\boldsymbol{x}+\boldsymbol{r})\rangle = \sum_{\boldsymbol{k}}\sum_{\boldsymbol{k}''}\langle \hat{f}(\boldsymbol{k})\hat{g}^*(\boldsymbol{k}'')\rangle e^{-i\boldsymbol{x}\cdot(\boldsymbol{k}-\boldsymbol{k}'')+i\boldsymbol{k}''\cdot\boldsymbol{r}} \ . \tag{9.55}$$

By orthogonality of the Fourier modes, we have the relation

$$\int e^{i(\boldsymbol{k}-\boldsymbol{k}')\cdot\boldsymbol{x}}d^3\boldsymbol{x} = \begin{cases} 0 & \text{if } \boldsymbol{k} \neq \boldsymbol{k}', \\ L^3 \text{ or } (2\pi)^3 & \text{if } \boldsymbol{k} = \boldsymbol{k}' , \end{cases} \tag{9.56}$$

and the Eq. (9.55) becomes with $\boldsymbol{k}'' = \boldsymbol{k}$

$$Q_{fg}(\boldsymbol{r}) = \sum_{\boldsymbol{k}}\langle \hat{f}(\boldsymbol{k})\hat{g}^*(\boldsymbol{k})\rangle e^{i\boldsymbol{k}\cdot\boldsymbol{r}} \ . \tag{9.57}$$

In the Fourier representation (9.57), we use again L as the size of the cubic box with $k_i = 2\pi n_i/L$, $n_i = 0, \pm 1, \pm 2, \dots$. If we let $L \to \infty$, the sums become integrals and one writes

$$Q_{fg}(\boldsymbol{r}) = \int \langle \hat{f}(\boldsymbol{k})\hat{g}^*(\boldsymbol{k})\rangle e^{i\boldsymbol{k}\cdot\boldsymbol{r}}d^3\boldsymbol{k} \ , \tag{9.58}$$

where $d^3\boldsymbol{k}$ denotes the elemental volume in Fourier space. Defining by $E_{fg}(\boldsymbol{k})$ the cospectrum of f and g as $\langle \hat{f}(\boldsymbol{k})\hat{g}^*(\boldsymbol{k})\rangle$, we obtain

$$E_{fg}(\boldsymbol{k}) = \frac{1}{(2\pi)^3}\int Q_{fg}(\boldsymbol{r})e^{-i\boldsymbol{k}\cdot\boldsymbol{r}}d^3\boldsymbol{r} \ . \tag{9.59}$$

One notices that Q_{fg} and E_{fg} are Fourier transforms of each other.

9.6.2 Velocity Correlations and Associated Spectra

Setting $f = v'_i$ and $g = v'_j$, we define the two-point velocity correlation tensor

$$Q_{ij}(\boldsymbol{r}) = \overline{v'_i(\boldsymbol{x})v'_j(\boldsymbol{x} + \boldsymbol{r})} \ . \tag{9.60}$$

When $f = g = v'_i$, this is the self-correlation function. For $\boldsymbol{r} = \boldsymbol{0}$, we have

$$Q_{ii}(\boldsymbol{0}) = \overline{v'_i(\boldsymbol{x})v'_i(\boldsymbol{x})} = 2K \ . \tag{9.61}$$

The velocity spectrum tensor $\boldsymbol{E}$ is thus the Fourier transform of Q_{ij}

$$E_{ij}(\boldsymbol{k}) = \frac{1}{(2\pi)^3} \int Q_{ij}(\boldsymbol{r})e^{-i\boldsymbol{k}\cdot\boldsymbol{r}}d^3\boldsymbol{r} \ . \tag{9.62}$$

Moreover,

$$Q_{ij}(\boldsymbol{r}) = \int E_{ij}(\boldsymbol{k})e^{i\boldsymbol{k}\cdot\boldsymbol{r}}d^3\boldsymbol{k} \ . \tag{9.63}$$

The Reynolds tensor τ_{ij} is obtained by

$$\tau_{ij} = Q_{ij}(\boldsymbol{0}) \ . \tag{9.64}$$

With (9.63), we have

$$\tau_{ij} = \int E_{ij}(\boldsymbol{k})d^3\boldsymbol{k} \ . \tag{9.65}$$

It is easily shown that $\boldsymbol{Q}$ possesses a symmetry such that

$$\boldsymbol{Q}(-\boldsymbol{r}) = \boldsymbol{Q}^T(\boldsymbol{r}) \ . \tag{9.66}$$

Consequently, the tensor $\boldsymbol{E}$ has the property

$$\boldsymbol{E}(-\boldsymbol{k}) = \boldsymbol{E}^T(\boldsymbol{k}) \ . \tag{9.67}$$

Let us introduce the general tensor

$$D_{ijpq} = \overline{\frac{\partial v'_i}{\partial x_p} \frac{\partial v'_j}{\partial x_q}} \ . \tag{9.68}$$

From the definition (9.60), one obtains

$$\frac{\partial Q_{ij}(\boldsymbol{r})}{\partial r_q} = \overline{v'_i(\boldsymbol{x})\frac{\partial v'_j(\boldsymbol{x} + \boldsymbol{r})}{\partial r_q}} \ . \tag{9.69}$$

Replacing $\boldsymbol{x}$ by $\boldsymbol{x}' - \boldsymbol{r}$ in (9.69) and taking the derivative with respect to r_p, we have

$$\frac{\partial^2 Q_{ij}(\boldsymbol{r})}{\partial r_p \partial r_q} = -\overline{\frac{\partial v_i'(\boldsymbol{x}' - \boldsymbol{r})}{\partial r_p} \frac{\partial v_j'(\boldsymbol{x}')}{\partial r_q}} . \tag{9.70}$$

Letting $\boldsymbol{r}$ go to zero, the tensor D_{ijpq} yields

$$D_{ijpq} = -\frac{\partial^2 Q_{ij}(\boldsymbol{r})}{\partial r_p \partial r_q} \mid_{\boldsymbol{r}=\boldsymbol{0}} . \tag{9.71}$$

Applying Eqs. (9.73) to (9.63), we find

$$D_{ijpq} = \int k_p k_q E_{ij}(\boldsymbol{k}) d^3 \boldsymbol{k} . \tag{9.72}$$

The dissipation rate ε (9.41) may be linked to the previous tensor by the relation

$$\varepsilon = \nu D_{iijj} . \tag{9.73}$$

With the Eqs. (9.72) and (9.73), we compute

$$\varepsilon = \nu \int k^2 E_{ii}(\boldsymbol{k}) d^3 \boldsymbol{k} . \tag{9.74}$$

With Eq. (9.61) the turbulent kinetic energy is expressed as

$$K = \frac{1}{2} tr \, \boldsymbol{Q}(\boldsymbol{0}) = \frac{1}{2} \int E_{ii}(\boldsymbol{k}) d^3 \boldsymbol{k} . \tag{9.75}$$

The k^2 factor in (9.74) shows that the main contribution to the dissipation comes from wave numbers higher than those characterizing the kinetic energy. This is a partial confirmation of the validity of Kolmogorov hypothesis for the energy cascade in homogeneous turbulence.

9.6.3   Correlations and Spectra in Isotropic Turbulence

In isotropic turbulence, the tensor $\boldsymbol{E}$ is an isotropic tensor function of only $k = \sqrt{\boldsymbol{k} \cdot \boldsymbol{k}}$. Its more general form is

$$\boldsymbol{E}(\boldsymbol{k}) = C_1 \boldsymbol{I} + C_2 \, \boldsymbol{k} \otimes \boldsymbol{k} . \tag{9.76}$$

The incompressibility condition (1.50) applied to the Fourier expansion of the velocity field

$$\boldsymbol{v}(\boldsymbol{x}) = \sum_{k} \hat{\boldsymbol{v}}(\boldsymbol{k})\, e^{-i\boldsymbol{k}\cdot\boldsymbol{x}} \tag{9.77}$$

imposes $k_j\,\hat{v}_j(\boldsymbol{k}) = 0$ such that the Fourier coefficients of the velocity must be orthogonal to $\boldsymbol{k}$. Therefore, we have

$$k_i\, E_{ij} = k_j\, E_{ij} = 0, \tag{9.78}$$

and thus, one obtains

$$C_1 k_j + C_2 k^2 k_j = 0 \tag{9.79}$$

and consequently

$$C_2 = -C_1/k^2 \ . \tag{9.80}$$

Redefining C_1 as

$$C_1 = \frac{E(k)}{4\pi k^2}, \tag{9.81}$$

(and that is justified by the isotropy in the spectral space with $dE = 4\pi k^2\, E(k)\, dk$ which gives the energy density between the spherical layers k and $k + dk$), we get

$$\boldsymbol{E}(\boldsymbol{k}) = \frac{E(k)}{4\pi k^2}\left(\boldsymbol{I} - \frac{\boldsymbol{k}\otimes\boldsymbol{k}}{k^2}\right) \ . \tag{9.82}$$

We call $E(k)$ the spectral energy function.

The turbulence energy via (9.75) and (9.82) becomes

$$K = \int \frac{1}{4\pi k^2} E(k)\, d^3\boldsymbol{k} \ . \tag{9.83}$$

This integral is computed in spherical coordinates as shown in Fig. 9.3.

We have

$$K = \frac{1}{4\pi} \int_{k=0}^{\infty} \int_{\theta=0}^{\pi} \int_{\phi=0}^{2\pi} \frac{E(k)}{k^2} k^2 \sin\theta\, d\theta\, d\varphi\, dk \ . \tag{9.84}$$

Integrating with respect to θ and φ, and because of the isotropy, we obtain

$$K = \int_0^{\infty} E(k)\, dk \ . \tag{9.85}$$

Let us note that $E(k)$ has dimension $m^3 s^{-2}$. In isotropic turbulence, the energy spectrum is completely determined as soon as $E(k)$ is specified.

As the $\boldsymbol{E}$ tensor is the Fourier transform of $\boldsymbol{Q}$ (Eq. (9.62)) in isotropic turbulence, the velocity correlation tensor is completely defined by two correlation functions (Fig. 9.4). The longitudinal correlation function
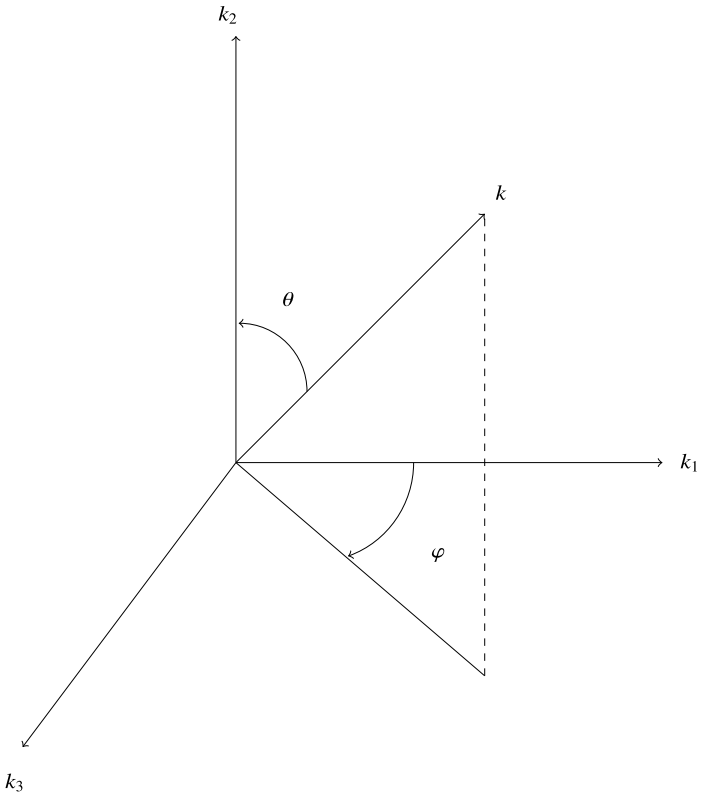
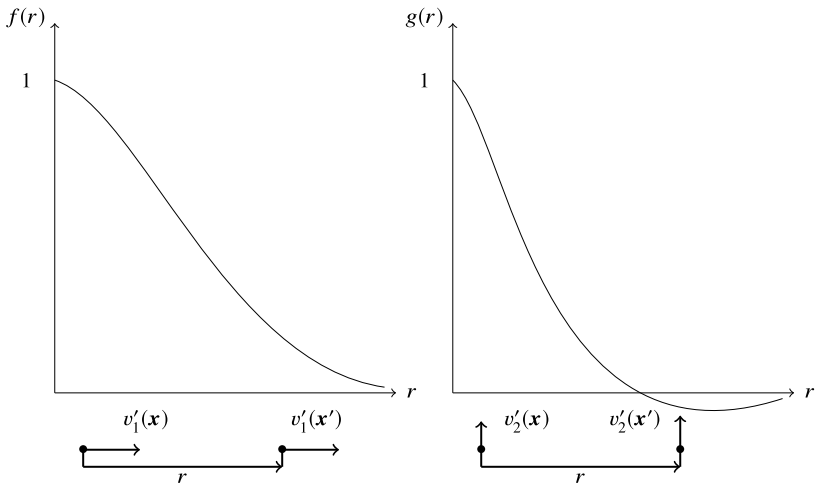**Fig. 9.3** Spherical coordinates for Fourier space integration

Fig. 9.4 Longitudinal and transverse correlations

$$f(r) = \frac{3}{2K} Q_{11}(r_1, 0, 0) \tag{9.86}$$

describes the coherence of fluctuations aligned in the direction of the vector separating the two points. The transverse correlation function

$$g(r) = \frac{3}{2K} Q_{22}(r_1, 0, 0) \tag{9.87}$$

is the image of the coherence of fluctuations of velocities orthogonal to the separation line. The most general expression of tensor $\mathbf{Q}$ is

$$\mathbf{Q}(\mathbf{r}) = C_1 \mathbf{I} + C_2 \mathbf{r} \otimes \mathbf{r} \tag{9.88}$$

with the definition

$$r = \sqrt{r_i r_i} \ . \tag{9.89}$$

The constants C_1 and C_2 are easily evaluated

$$Q_{22}(r_1, 0, 0) = \frac{2K}{3} g(r) = C_1,$$

$$Q_{11}(r_1, 0, 0) = \frac{2K}{3} f(r) = C_1 + C_2 r^2.$$

Solving this system, we find

$$\mathbf{Q}(r) = \frac{2K}{3} \left[\frac{f(r) - g(r)}{r^2} \mathbf{r} \otimes \mathbf{r} + g(r) \mathbf{I} \right] \ . \tag{9.90}$$

In this last expression, we note that the functions f and g are scalar functions of the (scalar) distance of separation.

In theory, homogeneous isotropic turbulence evolves with time and we should measure the spectral tensor by taking measurements in many points. In reality, this is very difficult. Therefore the experimenters use Taylor's hypothesis which assumes that the turbulence time history mirrors the space history as turbulence is only advected around the measurement device. We conclude that the measurement of $v_1'(\mathbf{x}, t)$ yields $Q_{11}(r_1, 0, 0, t)$. In other words, we replace time correlations by space correlations.

Inserting (9.82) in (9.63), we obtain

$$Q_{11}(r_1, 0, 0) = \int \frac{E(k)}{4\pi k^2} \left(1 - \frac{k_1^2}{k^2} \right) e^{ik_1 r_1} d^3 \mathbf{k} \ . \tag{9.91}$$

Referring to Fig. 9.5 for the Fourier wavenumber integration, we observe that k_1 wavenumbers contribute substantially. As k_1 goes from $-\infty$ to $+\infty$, these terms

have the imaginary parts of $e^{ik_1r_1}$ with opposite signs and therefore cancel each other
leaving only cosines in the integral. This integral reads now

$$Q_{11}(r_1, 0, 0) = \int_{k_1=0}^{\infty} \int_{k=k_1}^{\infty} \int_{\varphi=0}^{2\pi} \frac{E(k)}{4\pi k^2} \left(1 - \frac{k_1^2}{k^2}\right) 2\cos(k_1 r_1) k\, d\varphi\, dk\, dk_1 \ . \quad (9.92)$$

The φ integration gives 2π and we are left with

$$Q_{11}(r_1, 0, 0) = \int_{k=k_1}^{\infty} E_1(k_1)\cos(k_1 r_1) dk_1 \quad (9.93)$$

with the definition of the one-dimensional spectral function E_1

$$E_1(k_1) = \int_{k=k_1}^{\infty} \frac{E(k)}{k} \left(1 - \frac{k_1^2}{k^2}\right) dk \ . \quad (9.94)$$

With relation (9.93), we notice that the Fourier cosine transform of measurements
$Q_{11}(r_1, 0, 0)$ is an efficient tool to obtain $E_1(k_1)$. By taking twice the derivative of
Eq. (9.94) with respect to k_1, one has

$$E(k_1) = \frac{k_1^2}{2} \frac{\partial^2 E_1(k_1)}{\partial k_1^2} - \frac{k_1}{2} \frac{\partial E_1(k_1)}{\partial k_1} \ . \quad (9.95)$$

This equation allows to establish $E(k)$. Its general shape is shown in Fig. 9.2. By
(9.85), the surface beneath the curve gives the turbulent kinetic energy that receives
its maximum contribution from wave-numbers located near the maximum.

Fig. 9.6 Spectrum of the longitudinal fluctuation $\frac{E(k)}{\nu^{5/4}\varepsilon^{1/4}}$ with respect to the Kolmogorov variable $\frac{k\nu^{3/4}}{\varepsilon^{1/4}}$
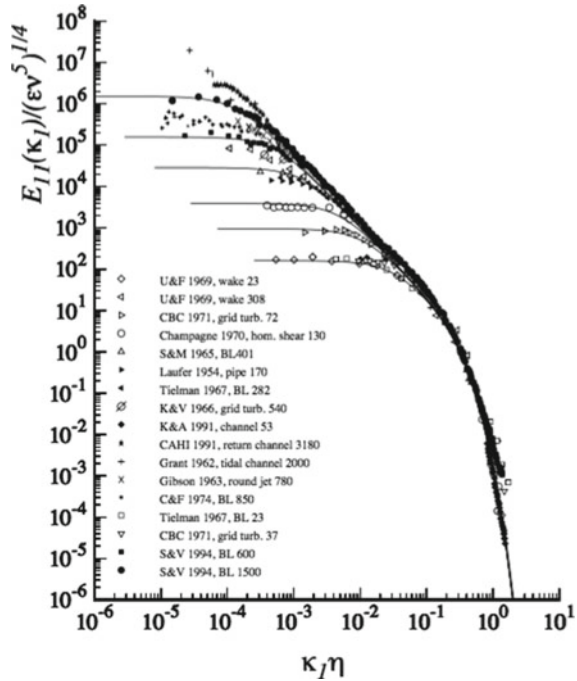
It is supposed that the small scale motions in every turbulent flow become isotropic for high Reynolds numbers and that the Kolmogorov scales characterize the region of large wave-numbers (or of small spatial scales) of any turbulent flow. If we suppose the existence of a universal spectrum at small scale, by means of dimensional analysis, we have

$$\frac{E(k)}{v_K^2 \ell_K} = \frac{E(k)}{\nu^{5/4}\varepsilon^{1/4}} = F(\ell_K k) = F\left(\frac{k\nu^{3/4}}{\varepsilon^{1/4}}\right) . \tag{9.96}$$

Figure 9.6 shows that the experimental data for a vast diversity of flows fall effectively on a common curve when Kolmogorov variables are used.

Kolmogorov [42, 43] suggests that there exists a wave-number range for which the dominant physical mechanism consists in transmitting the energy of the large structures towards the small scales (cascade) and that the structure of this region depends only on the speed of the energy transfer. This interval is called the inertial zone or else inertial range. Since this cascade ends with the small-scale dissipation, the transfer rate is equal to the dissipation rate ε. We assume, therefore, that $E(k)$ depends only on k and ε. Applying dimensional analysis, we get

$$E(k) = C\, \varepsilon^{2/3}\, k^{-5/3} . \tag{9.97}$$

This is Kolmogorov spectrum. Note that this result proved in homogeneous isotropic turbulence remains valuable in many non homogeneous and non isotropic turbulent configurations.

The correlation functions f and g give a certain idea of the turbulent motion. The integral scales are useful for the large scale motion. One can define for example:

$$L_{11}(t) = \frac{\int_0^t Q_{11}(r_1, 0, 0, t)dr_1}{Q_{11}(0, 0, 0, t)} \tag{9.98}$$

giving a measure of the size of the vortices in direction x_1. Another scale that is often used is Taylor's microscale λ_T. A possible definition is

$$\varepsilon = \nu \frac{K}{\lambda_T^2} . \tag{9.99}$$

If we compare Taylor's microscale to Kolmogorov scale, we have

$$\frac{\lambda_T}{\ell_K} = Re_T^{1/4} . \tag{9.100}$$

If we compare λ_T to the size of energetic structures (9.40), we obtain

$$\frac{\ell}{\lambda_T} = Re_T^{1/2} . \tag{9.101}$$

Thus, the microscale is comprised between the smallest and the largest scales.

9.7 Fourier Spectral Solution

The assumption of spatial homogeneity naturally leads to a Fourier representation of the primitive variables of the Navier–Stokes equations. In this case, the absence of solid walls eases the elaboration of solutions and the differential operators are replaced by wavenumber multiplications in spectral space. Nevertheless, these Fourier tools yield direct access to spectra that are convenient and reliable theoretical instruments to interpret the physical phenomena. As might be expected, the field has been extensively explored and exploited by several authors arguably starting with the monograph by Batchelor [11]. Over the intervening decades there have been several reviews and these are nicely highlighted by Lesieur [50] and McComb [54].

The velocity field is approximated by the following Fourier series given in a 2π periodic box

$$\boldsymbol{v}(\boldsymbol{x}, t) = \sum_{\boldsymbol{k}} \boldsymbol{u}(\boldsymbol{k}, t) \exp(i\boldsymbol{k} \cdot \boldsymbol{x}) , \tag{9.102}$$

where the wavevector $\boldsymbol{k} = (k_1, k_2, k_3)$ goes from $-\infty$ to ∞. The k_i are integers.

For the sake of facility, we rewrite the Navier–Stokes equations with the non-linear term in conservative form taking the incompressibility into account

$$\frac{\partial \boldsymbol{v}}{\partial t} + \boldsymbol{\nabla} \cdot (\boldsymbol{v} \otimes \boldsymbol{v}) = -\frac{1}{\rho} \boldsymbol{\nabla} p + \nu \triangle \boldsymbol{v} . \tag{9.103}$$

With (9.102), the Fourier representation of the tensor product appearing in the non-linear term is obtained as follows

$$\begin{aligned} (\boldsymbol{v} \otimes \boldsymbol{v})_{ij} = v_i v_j &= \sum_{\boldsymbol{k}'} u_i(\boldsymbol{k}', t) e^{i\boldsymbol{k}' \cdot \boldsymbol{x}} \sum_{\boldsymbol{k}''} u_j(\boldsymbol{k}'', t) e^{i\boldsymbol{k}'' \cdot \boldsymbol{x}} \\ &= \sum_{\boldsymbol{k}' + \boldsymbol{k}'' = \boldsymbol{k}} u_i(\boldsymbol{k}', t) u_j(\boldsymbol{k}'', t) e^{i(\boldsymbol{k}' + \boldsymbol{k}'') \cdot \boldsymbol{x}} . \end{aligned} \tag{9.104}$$

The pressure field is also given by a Fourier series such that

$$\frac{1}{\rho} p = \sum_{\boldsymbol{k}} \hat{p}(\boldsymbol{k}, t) \exp(i\boldsymbol{k} \cdot \boldsymbol{x}) . \tag{9.105}$$

The insertion of the Fourier approximations of the various terms in (9.103), followed by the multiplication of the resulting relation by $e^{-i\boldsymbol{k} \cdot \boldsymbol{x}}$ and then integration on the periodic cube leads to the equation

$$\frac{du_i}{dt} + \nu k^2 u_i = -ik_i \hat{p} - C_i , \tag{9.106}$$

where C_i is the non-linear convective term which in Fourier space is given by

$$C_i = ik_m \sum_{\boldsymbol{k}' + \boldsymbol{k}'' = \boldsymbol{k}} u_i(\boldsymbol{k}', t) u_m(\boldsymbol{k}'', t) . \tag{9.107}$$

Taking the divergence of (9.106) with the incompressibility constraint, we get the pressure Poisson equation

$$k^2 \hat{p} = ik_i C_i . \tag{9.108}$$

The pressure $\hat{p}$ is then

$$\hat{p} = i \frac{k_l}{k^2} C_l . \tag{9.109}$$

The dynamical Navier–Stokes equation (9.106) becomes

$$\left(\frac{d}{dt} + \nu k^2\right) u_i = \frac{k_i k_l}{k^2} C_l - C_i$$
$$= -(\delta_{il} - \frac{k_i k_l}{k^2}) C_l$$
$$= -P_{il} C_l \,, \tag{9.110}$$

with $P_{il} = \delta_{il} - k_i k_l / k^2$, the projection tensor of the velocity field on a plane that is orthogonal to the $\boldsymbol{k}$ vector.

It is very often preferred to write (9.110) in symmetric form, i.e. in terms of the compound projection operator P_{ilm}

$$P_{ilm} = k_l P_{im} + k_m P_{il} \,, \tag{9.111}$$

such that

$$\left(\frac{d}{dt} + \nu k^2\right) u_i = -\frac{i}{2} P_{ilm} \sum_{\boldsymbol{k}'+\boldsymbol{k}''=\boldsymbol{k}} u_l(\boldsymbol{k}', t) u_m(\boldsymbol{k}'', t) \,, \tag{9.112}$$
$$k_i u_i = 0 \,. \tag{9.113}$$

Equations (9.112) and (9.113) are amenable to numerical Fourier spectral approximation if we apply a cut-off wavenumber k_c in the $\boldsymbol{k}$ space in such a way that $\|\boldsymbol{k}\| < k_c$. In the convolution term, $\|\boldsymbol{k}'\| < k_c$ and $\|\boldsymbol{k}''\| < k_c$, cf. S. A. Orszag [67].

Even though the numerical integration is carried out in spectral space, the non-linearity is computed in physical space by so-called pseudo-spectral or more appropriately collocation method. The passage between Fourier and physical space and vice-versa is performed by discrete Fourier transforms (DFT). All derivatives are accurately computed in spectral space. For the non-linear terms the various contributions are transformed in physical space by DFT on the collocation grid, where the product $\boldsymbol{v} \cdot \boldsymbol{\nabla} \boldsymbol{v}$ is evaluated at these nodes and transformed back to Fourier space by inverse DFTs. Dealiasing procedures are needed to avoid spectral pollution in the high wave numbers.

9.8   Linear Turbulence Models

The real life applications are very seldom taking place in periodic geometries. Engineering practice implies complicated internal or external shapes and the presence of walls renders matters quite complex. Therefore a number of approaches of turbulent flows require the use of turbulent models following the lead of Lumley [52] and more recently Gatski [33]. We review some of them in the next subsections.

9.8.1 Zero Equation Model

This closure scheme is often called algebraic to clearly demonstrate the fact that there is no transport equation to describe the Reynolds stresses, but only algebraic expressions relating them to the velocity field $\overline{v}(x)$. By analogy with the viscous Newtonian fluid model, we write the constitutive turbulent equation for the Reynolds stress as

$$\boldsymbol{R} = 2\mu_T \overline{\boldsymbol{d}} \, , \tag{9.114}$$

using the turbulent (dynamic) viscosity μ_T. This turbulent viscosity was introduced by Boussinesq [17]. It should be emphasized that we reason by analogy with the mechanics of continuous media where we deduce equations for the viscous Newtonian fluid. Here, however, we do not characterize a material behavior but the state of a flow. In order to ensure a correct writing of the Reynolds tensor, we write the Eq. (9.114) in the form:

$$\boldsymbol{\tau} - \frac{2K}{3}\boldsymbol{I} = -2\nu_T \overline{\boldsymbol{d}} \, . \tag{9.115}$$

The addition of the diagonal term allows to obtain in the left hand side a tensor with a zero trace as is $\overline{\boldsymbol{d}}$ and $\tau_{ii} = 2K$. The turbulent viscosity is fixed by K, ε and ℓ, the mixing length. By dimensional analysis, we have

$$\nu_T \simeq K^{1/2}\ell \quad \text{or} \quad \nu_T \simeq K^2/\varepsilon = \tau K \, , \tag{9.116}$$

where τ is the turbulent velocity time.

9.8.2 Turbulent Flow in a Plane Channel

Here we deal with the case of a particular flow that will enable us to write with full details the closure problem described by Eqs. (9.115)–(9.116). We consider a statistically steady state flow between two parallel planes of infinite horizontal extension that constitute a channel of height $2h$. The mean flow is a pure shear flow, homogeneous in direction x_1, such that

$$\overline{\boldsymbol{v}} = (\overline{v_1}(x_2), 0, 0) \, . \tag{9.117}$$

The Eqs. (9.14) of the mean motion become

$$0 = -\frac{\partial \overline{p}}{\partial x_1} + \mu \frac{\partial^2 \overline{v_1}}{\partial x_2^2} + \frac{\partial}{\partial x_2}(-\rho \, \overline{v_1' v_2'}), \tag{9.118}$$

$$0 = -\frac{\partial \overline{p}}{\partial x_2} + \frac{\partial}{\partial x_2}(-\rho \, \overline{v_2'^2}), \tag{9.119}$$

$$\frac{\partial \overline{v_1}}{\partial x_1} = 0 \,. \tag{9.120}$$

Integrating (9.119) yields

$$\overline{p} + \rho \overline{v_2'^2} = p_0(x_1) \,. \tag{9.121}$$

We may rewrite (9.118) as

$$\frac{\partial}{\partial x_2}(\mu \frac{\partial \overline{v_1}}{\partial x_2} - \rho \, \overline{v_1' v_2'}) = \frac{dp_0}{dx_1} = -A \,. \tag{9.122}$$

As the left hand side can only be a function of x_2 because of the hypotheses of steady state homogeneous turbulence and as the right hand side is only function of x_1, each side must be equal to a constant. One gets

$$\mu \frac{\partial \overline{v_1}}{\partial x_2} - \rho \, \overline{v_1' v_2'} = -Ax_2 + B \,. \tag{9.123}$$

In the left hand side, we have the total stress resulting from the viscous and Reynolds stresses. If the origin of the axes is located at mid-height of the channel, by symmetry, B must vanish in $x_2 = 0$.

Let us move the origin of the coordinate system on the lower wall. We assume that the mixing length increases linearly with the distance to the wall, i.e.

$$\ell = \kappa x_2 \,. \tag{9.124}$$

The vortices close to a wall have a characteristic dimension proportional to the wall distance. Let us note that turbulence is zero on this wall by the no-slip condition.

Using the model of turbulent viscosity (9.115) and assuming a steady state homogeneous turbulence, one obtains with (9.22)

$$\mathcal{P} = \mathcal{D}, \tag{9.125}$$

and

$$\mathcal{P} = 2\nu_T \overline{d}_{ij} \overline{d}_{ij} = \varepsilon \,. \tag{9.126}$$

By (9.40), (9.116) and (9.126), we eliminate $K^{1/2}$ and ε. We have

$$\begin{aligned} \nu_T &\approx K^{1/2} \ell = \varepsilon^{1/3} \ell^{4/3} \\ &= (2\nu_T \overline{d}_{ij} \overline{d}_{ij})^{1/3} \ell^{4/3} \end{aligned} \tag{9.127}$$

and therefore

$$\nu_T \approx \ell^2 (2\overline{d}_{ij}\overline{d}_{ij})^{1/2} \ . \tag{9.128}$$

For the flow between two parallel walls, we have $\overline{d}_{12} = \overline{d}_{21}$ and then,

$$\nu_T = \ell^2 \frac{\partial \overline{v_1}}{\partial x_2} \ . \tag{9.129}$$

9.8.3   The Logarithmic Velocity Profile

Combining (9.115), (9.123) and (9.129), we obtain

$$\left(\mu + \rho\ell^2 \frac{\partial \overline{v_1}}{\partial x_2}\right)\frac{\partial \overline{v_1}}{\partial x_2} = -Ax_2 + B \ , \tag{9.130}$$

where B is the wall shear stress that we denote τ_w. In the neighborhood of the wall assumed to be smooth, the turbulent exchanges are negligible with respect to the molecular viscosity effects. We are in the viscous sub-layer. The Eq. (9.130) reduces to:

$$\mu \frac{\partial \overline{v_1}}{\partial x_2} = \tau_w = \rho v_*^2, \quad | Ax_2 | \ll B \ , \tag{9.131}$$

with v_*, the friction velocity. The velocity profile is linear

$$\frac{\overline{v_1}}{v_*} = \frac{v_* x_2}{\nu} = Re_* \ . \tag{9.132}$$

In (9.132), Re_* is the wall Reynolds number.

Beyond the viscous sub-layer, we neglect the molecular diffusion with respect to the turbulent diffusion. The relation (9.130) with (9.124) becomes:

$$\rho\kappa^2 x_2^2 \left(\frac{d\overline{v_1}}{dx_2}\right)^2 = -Ax_2 + B \ . \tag{9.133}$$

The integration of this non-linear differential equation is not simple. We notice experimentally that the result obtained for $x_2/h < 0.2$ is very close to that obtained when Ax_2 is neglected compared to B. Consequently, in this zone, the shear stress remains constant. We have the relation:

$$\frac{d\overline{v_1}}{dx_2} = \frac{v_*}{\kappa x_2} \ . \tag{9.134}$$

Integrating Eq. (9.134) yields

$$\overline{v_1} = \frac{v_*}{\kappa} \log x_2 + C \ . \tag{9.135}$$

To know the velocity variation close to the wall, we need to determine the value of the integration constant C. To this end, we will admit that the velocity $\overline{v_1}$ vanishes, at a distance from the wall corresponding to the thickness δ_s of the viscous sub-layer. We set the condition:

$$\overline{v_1} = 0 \quad \text{in} \quad x_2 = \delta_s = \beta \frac{v}{v_*} \ , \tag{9.136}$$

β being a numerical constant. This way to express the thickness δ_s is classically adopted in order to get the wall distance x_2 dimensionless using the wall Reynolds number Re_*:

$$\frac{v_* x_2}{v} = Re_* \ . \tag{9.137}$$

Condition (9.136) applied to (9.135) yields

$$C = -\frac{v_*}{\kappa} \log \frac{\beta v}{v_*} \ . \tag{9.138}$$

The relation (9.135), with C given by (9.138), is written as:

$$\frac{\overline{v_1}}{v_*} = \frac{1}{\kappa} (\log \frac{x_2 v_*}{v} - \log \beta) = \frac{1}{\kappa} (\log Re_* - \log \beta) \ . \tag{9.139}$$

The experimental data show that κ, the von Kármán constant, has a value independent on the wall nature (rough or smooth) and is equal to 0.4. On the other hand, the β value, that is in the mean of the order of 0.1, is influenced by the wall roughness.

The logarithmic profile (9.139) is one of the most celebrated results of turbulence theory. Figure 9.7 is a semi-log plot. The straight line corresponding to Eq. (9.139) is obvious. When $x_2 v_*/v$ is <30, the molecular viscosity becomes important in this zone. The laminar stresses are dominant and the turbulent stresses are negligible, allowing to write the next equalities:

$$\tau_{12} = \mu \frac{\partial \overline{v_1}}{\partial x_2} = \tau_w = \rho v_*^2 \tag{9.140}$$

or

$$\frac{\overline{v_1}}{v_*} = \frac{v_* x_2}{v} = Re_* \ . \tag{9.141}$$

The curve corresponding to this profile is included in Fig. 9.7. The experimental data are in good agreement for $x_2 v_*/v < 8$. For $x_2/h > 0.2$, the logarithmic law no longer fits exactly the experimental results. In the region between $x_2/h = 0.2$ and
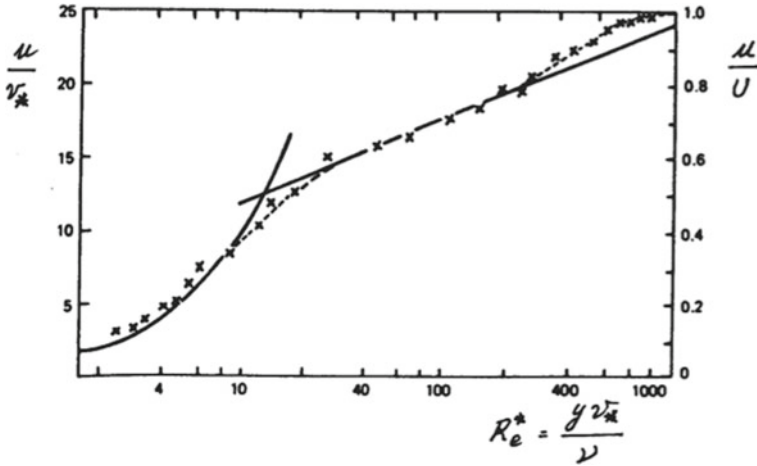
Fig. 9.7 Logarithmic velocity profile in a turbulent boundary layer with $u = v_1$, $y = x_2$. Crosses are experimental data

$x_2/h = 1$, one uses the wake function. The profile is then the logarithmic relation plus a function $w(x_2/\delta)$ with δ a characteristic thickness of the problem. One obtains

$$\frac{\overline{v_1}(x_2)}{v_*} = \frac{1}{\kappa} \log \frac{v_* x_2}{\nu} + C + \frac{1}{\kappa} \Pi w(\frac{x_2}{\delta}) \tag{9.142}$$

with

$$w = 2 \sin^2(\frac{x_2}{\delta} \frac{\pi}{2}) . \tag{9.143}$$

The parameter Π is linked to the pressure gradient. In a boundary layer with constant pressure, $\Pi = 0.6$. For a pipe flow, $\Pi = 1/4$ with $\delta = R$.

9.9   The One-Equation Model: the $K - \ell$ Model

The algebraic closure of the zero equation model is often criticized for two reasons. The first one notices that there exists a number of flow experiments where $\overline{d}$ and $\overline{v' \otimes v'}$ do not change sign at the same location. Therefore, the turbulent viscosity could be negative and this is physically not expected. However, experimentally the regions where the turbulent viscosity is negative, are spatially small in most industrial applications so that the local failure of this model has no major consequence.

The second reason consists in that the relationship between $\overline{d}$ and $\overline{v' \otimes v'}$ is purely local, ignoring de facto the "history" of turbulence. In order to improve this situation, one adds a transport equation for a relevant velocity scale of the turbulent motion. The most significant scale from the physical point of view is $K^{1/2}$, cf. (9.20). With

the Eqs. (9.22) and (9.23) of the turbulent kinetic energy, we observe that we have generated new correlations in the diffusion and dissipation terms. In order to close the system of equations, the $K - \ell$ model introduces the following hypotheses. One replaces the first two terms of the turbulent kinetic energy flux (9.23) by a gradient and one develops a link between the dissipation rate ε and the kinetic energy by an algebraic relation. One gets

$$- \left(\frac{1}{\rho} \overline{p' \boldsymbol{v}'} + \overline{\frac{1}{2}(\boldsymbol{v}' \cdot \boldsymbol{v}') \boldsymbol{v}'} \right) = \frac{\nu_T}{\sigma_q} \boldsymbol{\nabla} K \tag{9.144}$$

$$\varepsilon = \frac{C_D}{\ell} K^{3/2} \ , \tag{9.145}$$

with σ_q and C_D empirical constants. Usually, one sets $C_D = 0.164$. Similarly, one chooses μ_T as:

$$\mu_T = \rho K^{1/2} \ell \ , \tag{9.146}$$

where the mixing length ℓ is determined again by an algebraic relation. For completeness, it is worth noting that an alternative approach to determining the eddy viscosity is to solve a transport equation directly for the eddy viscosity ν_T (Spalart and Allmaras [94]). Such a one-equation model, though based primarily on empiricism and on dimensional analysis, is popular among industrial users, especially in aerodynamics and in turbomachinery, due to its ease of implementation and relatively inexpensive cost.

For three-dimensional flows, the concept of mixing length (9.124) can be generalized. With the gradient velocity tensor we have the Eq. (9.128) or if we use the vorticity

$$\nu_T = \ell^2 (\overline{\boldsymbol{\omega}} \cdot \overline{\boldsymbol{\omega}})^{1/2} \ , \tag{9.147}$$

where $\overline{\boldsymbol{\omega}} = \mathbf{curl}\ \overline{\boldsymbol{v}}$ is the average vorticity. This is the Baldwin–Lomax mixing length model [7].

Consequently, the governing equation of the $K - \ell$ model reads:

$$\frac{\partial K}{\partial t} + \overline{\boldsymbol{v}} \cdot \boldsymbol{\nabla} K = \boldsymbol{\nabla} \cdot \left((\nu + \frac{\nu_T}{\sigma_K}) \boldsymbol{\nabla} K \right) + 2\nu_T \, \overline{\boldsymbol{d}} : \boldsymbol{\nabla} \overline{\boldsymbol{v}} - C_D \frac{K^{3/2}}{\ell} \ . \tag{9.148}$$

Very often one sets σ_K equal to 1. This practice produces good results for various types of flows. To solve (9.148) the boundary condition imposes a vanishing K value on solid walls and a zero normal gradient on inflow and outflow sections.

9.10 The Two-Equation Models

In this section we will look at the widely used $K - \varepsilon$ and $K - \omega$ models. These approaches try to circumvent the deficiencies of the one-equation modeling by the addition of a second partial differential equation. Both models use (9.115) for the Reynolds stress tensor.

9.10.1 $K - \varepsilon$ Model

One takes the derivative of the dynamic equation for the velocity fluctuations (9.19) with respect to x_l. Then, one multiplies the resulting equation by $\partial v_i' / \partial x_l$. This last relation is averaged. We obtain

$$
\frac{\partial}{\partial t} \frac{1}{2} \overline{\left(\frac{\partial v_i'}{\partial x_l}\right)^2} + \frac{\partial^2 \overline{v_i}}{\partial x_l \partial x_j} \overline{v_j' \frac{\partial v_i'}{\partial x_l}} + \frac{\partial \overline{v_i}}{\partial x_j} \overline{\frac{\partial v_i'}{\partial x_l} \frac{\partial v_j'}{\partial x_l}} + \frac{\partial \overline{v_j}}{\partial x_l} \overline{\frac{\partial v_i'}{\partial x_l} \frac{\partial v_i'}{\partial x_j}}
$$
$$
+ \overline{v_j} \frac{\partial}{\partial x_j} \frac{1}{2} \overline{\left(\frac{\partial v_i'}{\partial x_l}\right)^2} + \overline{\frac{\partial v_i'}{\partial x_l} \frac{\partial v_j'}{\partial x_l} \frac{\partial v_i'}{\partial x_j}} + \overline{v_j' \frac{\partial}{\partial x_j} \frac{1}{2} \left(\frac{\partial v_i'}{\partial x_l}\right)^2}
$$
$$
= -\frac{1}{\rho} \overline{\frac{\partial v_i'}{\partial x_l} \frac{\partial^2 p'}{\partial x_l \partial x_i}} + \nu \overline{\frac{\partial v_i'}{\partial x_l} \left(\frac{\partial^2}{\partial x_j^2} \left(\frac{\partial v_i'}{\partial x_l}\right)\right)} . \tag{9.149}
$$

Defining the dissipation rate ε

$$
\varepsilon = \nu \overline{\frac{\partial v_i'}{\partial x_l} \frac{\partial v_i'}{\partial x_l}} , \tag{9.150}
$$

we write Eq. (9.149) as follows

$$
\frac{\partial \varepsilon}{\partial t} + \overline{v_k} \frac{\partial \varepsilon}{\partial x_k} = \frac{\partial}{\partial x_k} \left(\nu \frac{\partial \varepsilon}{\partial x_k} - \nu \overline{v_k' \frac{\partial v_i'}{\partial x_l} \frac{\partial v_i'}{\partial x_l}} - 2\frac{\nu}{\rho} \overline{\frac{\partial p}{\partial x_i} \frac{\partial v_k'}{\partial x_i}} \right)
$$
$$
-2\nu \frac{\partial \overline{v_i}}{\partial x_k} \left(\overline{\frac{\partial v_i'}{\partial x_l} \frac{\partial v_k'}{\partial x_l}} + \overline{\frac{\partial v_l'}{\partial x_i} \frac{\partial v_l'}{\partial x_k}} \right) - 2\nu \overline{v_k' \frac{\partial v_i'}{\partial x_l}} \frac{\partial}{\partial x_k} \left(\frac{\partial \overline{v_i}}{\partial x_l} \right)
$$
$$
-2\nu \overline{\frac{\partial v_i'}{\partial x_l} \frac{\partial v_k'}{\partial x_l} \frac{\partial v_i'}{\partial x_k}} - 2\nu^2 \overline{\left(\frac{\partial}{\partial x_k} \left(\frac{\partial v_i'}{\partial x_l} \right) \right)^2} . \tag{9.151}
$$

On the left hand side of (9.151), we find the material derivative of the dissipation rate. Then in the first expression on the right hand side we have several diffusion terms: molecular, turbulent by velocity fluctuations, turbulent by pressure fluctuations. The two terms of the second line shows the production by the mean velocity gradients indicating the interaction between the turbulence and the mean flow. The penultimate

term in the third line shows the interaction between the gradients of the velocity fluctuations. Finally the last term is the dissipation of ε.

The Eq. (9.151) is often rewritten on the basis of empirical rather than theoretical considerations in the form

$$\frac{\partial \varepsilon}{\partial t} + \overline{\boldsymbol{v}} \cdot \nabla \varepsilon = \nabla \cdot \left((\nu + \frac{\nu_T}{\sigma_\varepsilon}) \nabla \varepsilon \right) + 2 C_{\varepsilon_1} \frac{\varepsilon}{K} \nu_T \, \overline{\boldsymbol{d}} : \overline{\boldsymbol{d}} - C_{\varepsilon_2} \frac{\varepsilon^2}{K} , \qquad (9.152)$$

where the eddy viscosity is defined as

$$\nu_T = C_\mu \frac{K^2}{\varepsilon} . \qquad (9.153)$$

Observe the strong similarity of Eqs. (9.148) and (9.152).

There has been many attempts to obtain the numerical values for the constants appearing in the $K - \varepsilon$ model by a careful analysis of the experimental data. However a convincing theoretical approach is based on the renormalization group theory (RNG) proposed by Yakhot and Orszag [123]. The RNG theory is well beyond of the scope of this monograph and we refer the reader to the available literature. The constants are given by Yakhot et al. [124]

$$C_{\varepsilon_1} = 1.42 \quad C_{\varepsilon_2} = 1.68 \quad \sigma_\varepsilon = \sigma_K = 0.719 \quad C_\mu = 0.0845 . \qquad (9.154)$$

The boundary conditions for K are identical to those proposed for the one-equation model. However for the two-equation approach, the appearance of ε induces complications to set up the boundary condition for that variable on the wall as its evaluation is rather tricky. The numericists and modelers resort to wall functions whereby the boundary conditions are not applied directly on the wall but at the beginning of the turbulent region close to the boundary. In the turbulent boundary layer, Eq. (9.126) yields

$$\nu_T \left(\frac{\partial \overline{v_1}}{\partial x_2} \right)^2 = \varepsilon . \qquad (9.155)$$

We also know that in the turbulent boundary layer, the shear stress is constant

$$\mu_T \left(\frac{\partial \overline{v_1}}{\partial x_2} \right) = \tau_w . \qquad (9.156)$$

Combining (9.155) and (9.156) with $\tau_w = \rho v_*^2$, we find

$$K = \frac{v_*^2}{\sqrt{C_\mu}} . \qquad (9.157)$$

The dissipation rate is obtained from (9.156) and the velocity profile (9.139)

$$\varepsilon = \frac{\mid v_* \mid^3}{\kappa x_2} \, .$$ (9.158)

Sometimes, Neumann type conditions are needed

$$\frac{\partial K}{\partial n} = 0, \quad v_* = (K_w)^{1/2} C_\mu^{1/4} \, ,$$ (9.159)

where K_w is the wall turbulence kinetic energy and $\partial/\partial n$ the normal derivative.

9.10.2 $K - \omega$ Model

In this model proposed by Wilcox [119, 120], K is still the turbulent kinetic energy while ω is the specific rate of dissipation of K, also referred to as the average frequency of the turbulence. The definition of ω is given as

$$\omega = \frac{\varepsilon}{K} \, .$$ (9.160)

The dimension of ω is indeed the inverse of time. The kinematic eddy viscosity is defined as

$$\nu_T = \frac{K}{\omega} \, .$$ (9.161)

The dynamic equation for ω may be obtained easily by formally dividing the variable in (9.148) by K and multiplying by ω yielding

$$\frac{\partial \omega}{\partial t} + \overline{v} \cdot \nabla \omega = \nabla \cdot \left((\nu + \frac{\nu_T}{\sigma_\omega}) \nabla \omega \right) + 2\alpha \nu_T \frac{\omega}{K} \overline{d} : \nabla \overline{v} - \beta \omega^2 \, .$$ (9.162)

The constants have the following values $\alpha = 5/9, \beta = 3/40, \sigma_\omega = 1/2$.

Two important topics have played a central role in the formulation of recent models of the Reynolds stresses: realizability and objectivity. Realizability imposes that the tensor diagonal components be individually positive

$$R_{\alpha\alpha} \geq 0, \quad \alpha = 1, 2, 3,$$ (9.163)

the greek index α indicating that there is no summation on the repeated indices in this case. Objectivity is a more delicate topic and is beyond the framework of this monograph [21, 95].

9.11   Non-linear Turbulence Models

So far we have examined linear turbulence models. However the physical reality of turbulence, as it is generated by the non-linear terms of the Navier–Stokes equations, is definitely non-linear. Therefore in this section we will tackle the construction of non-linear models to be able to cope better with the experimental data and the knowledge of turbulent phenomena. The two-equation models present the following defects: firstly, the inability to take into account the curvature effects of the streamlines and the deformations due to rotation; secondly, the neglect of non-local effects and history on the anisotropy of the Reynolds stresses.

9.11.1   Anisotropy Tensor

The anisotropy tensor of the Reynolds tensor is defined by the relationship

$$b_{ij} = \frac{\tau_{ij} - \frac{2K}{3}\delta_{ij}}{2K} \, , \tag{9.164}$$

and describes the deviations with respect to the isotropic situation. This tensor offers interesting properties. We notice that its trace which is the first invariant I_1

$$b_{ii} = I_1(\boldsymbol{b}) = 0 \tag{9.165}$$

is zero by Eq. (9.21). Most of the time, the use of the anisotropy tensor is related to its eigenvectors because then, the tensor is diagonal. As a consequence of (9.165) the sum of its eigenvalues vanish in such a way that only two such quantities are independent. Therefore the anisotropy is characterized by two independent invariants

$$I_2(\boldsymbol{b}) = -b_{ij}b_{ji}/2 = -\frac{1}{2}\operatorname{tr}\boldsymbol{b}^2, \quad I_3(\boldsymbol{b}) = b_{ij}b_{jk}b_{ki}/3 = \det\boldsymbol{b} \, . \tag{9.166}$$

If the turbulence is two-dimensional, because one velocity component in the direction of one of the principal axes always vanishes, we obtain

$$b_{\alpha\alpha} = -1/3 \quad \text{if} \quad \tau_{\alpha\alpha} = 0 \, . \tag{9.167}$$

There is no summation on Greek indices. If now all the energy is concentrated in a single component, we have

$$b_{\alpha\alpha} = 2/3 \quad \text{if} \quad \tau_{\alpha\alpha} = 2K \, . \tag{9.168}$$

This last case is named one-dimensional turbulence. We conclude that the eigenvalues of $\boldsymbol{b}$ are contained in the interval $[-1/3, 2/3]$.

Fig. 9.8 Anisotropy
invariant map.
$1D$-axisymmetric boundary
at $(I_3, -I_2) = (2/27, 1/3)$;
$2D$-axisymmetric boundary
at
$(I_3, -I_2) = (-1/108, 1/12)$
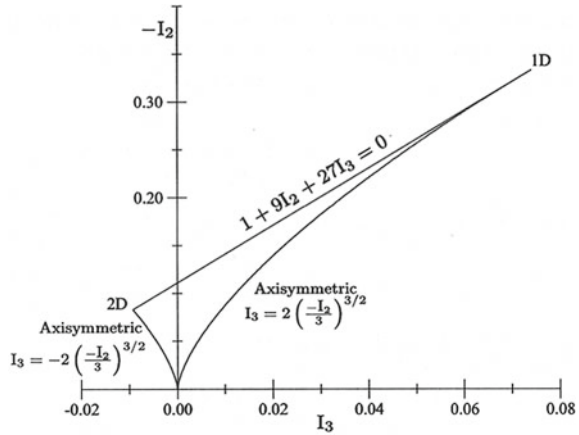
Lumley [53] examined the limiting values associated with b_{ij} in incompressible flows. For isotropic turbulence, the anisotropies vanish and the corresponding point is the origin in the anisotropy invariant map defined with the axes $(I_3, -I_2)$. From the origin, two other limiting boundaries are associated with axisymmetric turbulence where two of the diagonal elements are equal and the third is the negative sum of the other two (incompressibility). For example the anisotropy tensor in the principal coordinates is given by

$$b_{ij} = \text{diag}(a, a, -2a) . \tag{9.169}$$

We compute

$$I_2 = -3a^2, \quad I_3 = -2a^3 . \tag{9.170}$$

For $a > 0$, we have $I_3 = +(-2I_2/3)^{3/2}$, corresponding to an axisymmetric expansion. When $a < 0$, $I_3 = -(-2I_2/3)^{3/2}$ that corresponds to an axisymmetric contraction.

As Fig. 9.8 shows, a straight line connects the one-component axisymmetric limit with the two-component axisymmetric limit. This turbulence case corresponds to a Reynolds tensor with only two non zero components

$$\tau_{ij} = \text{diag}(0, p, q) , \tag{9.171}$$

with p, q both positive and $p + q = 2K$. Now let us set $q = K(1 - a/3)$, with $0 \le a \le 3$. We have successively

$$\tau_{ij} = \text{diag}(0, K(1 + a/3), K(1 - a/3))) \tag{9.172}$$

and the anisotropy tensor reads

$$b_{ij} = \text{diag}(0, (1 + a)/6, (1 - a)/6) . \tag{9.173}$$

The invariants are

$$I_2(\boldsymbol{b}) = -\frac{1}{12}\left(1 + \frac{a^2}{3}\right) , \quad I_3(\boldsymbol{b}) = \frac{a^2 - 1}{108} \tag{9.174}$$

For $a = 0$, $I_3(\boldsymbol{b}) = -1/108$ and with $a = 3$, $I_3(\boldsymbol{b}) = 2/27$.

Theorem 9.1 (Cayley–Hamilton theorem) *The Cayley–Hamilton theorem specifies that every tensor $\boldsymbol{b}$ satisfies its own characteristic equation*

$$\boldsymbol{b}^3 - I_1\boldsymbol{b}^2 + I_2\boldsymbol{b} - I_3\boldsymbol{I} = 0 . \tag{9.175}$$

In our case, (9.175) reduces to

$$b_{ij}^3 + I_2 b_{ij} - I_3 \delta_{ij} = 0 . \tag{9.176}$$

Using (9.176) with (9.174), the straight line of Fig. 9.8 is given by the relation

$$1 + 9I_2 + 27I_3 = 0 . \tag{9.177}$$

Referring to Eq. (9.115) for the Reynolds stress, the anisotropy tensor yields

$$\boldsymbol{b} = \frac{-2\nu_T \overline{\boldsymbol{d}}}{2K} . \tag{9.178}$$

This relation shows that the principal axes of the stress and the averaged strain rate are aligned. However this is not true for a particularly important engineering application, namely shear flows.

9.11.2 Dynamic Equation for the Anisotropy Tensor

In this section, we will resort to the index notation for ease of mathematical developments. The dynamic equation for the Reynolds stress (9.29) reads

$$\frac{D\tau_{ij}}{Dt} = -\tau_{ik}\frac{\partial \overline{v}_j}{\partial x_k} - \tau_{jk}\frac{\partial \overline{v}_i}{\partial x_k} + \Pi_{ij} - \varepsilon_{ij} + \mathcal{D}_{ij} , \tag{9.179}$$

where the various terms are

$$\Pi_{ij} = \overline{p'\left(\frac{\partial v'_i}{\partial x_j} + \frac{\partial v'_j}{\partial x_i}\right)} \tag{9.180}$$

$$\varepsilon_{ij} = 2\nu\overline{\frac{\partial v'_i}{\partial x_k}\frac{\partial v'_j}{\partial x_k}} \tag{9.181}$$

$$\mathcal{D}_{ij} = -\frac{\partial C_{ijk}}{\partial x_k}$$

$$= -\frac{\partial}{\partial x_k}\left(\overline{v'_i v'_j v'_k} + \overline{p'v'_i}\delta_{jk} + \overline{p'v'_j}\delta_{ik} - \nu\frac{\partial \tau_{ij}}{\partial x_k}\right) . \tag{9.182}$$

By incompressibility $\Pi_{ii} = 0$. Evaluating the trace of (9.179) leads to the dynamic equation of the turbulent energy

$$\frac{DK}{Dt} = \mathcal{P} - \varepsilon + \mathcal{D} , \tag{9.183}$$

where

$$\mathcal{P} = -\tau_{ik}\frac{\partial \overline{v}_i}{\partial x_k}, \quad \varepsilon = \frac{\varepsilon_{ii}}{2}, \quad \mathcal{D} = \frac{\mathcal{D}_{ii}}{2} . \tag{9.184}$$

Taking (9.179) and (9.183) into account, we obtain

$$\frac{Db_{ij}}{Dt} = \frac{1}{2K}\left(\frac{D\tau_{ij}}{Dt} - \frac{\tau_{ij}}{K}\frac{DK}{Dt}\right) . \tag{9.185}$$

Defining the anisotropy tensor for the dissipation-rate correlation

$$d_{ij} = \frac{\varepsilon_{ij} - \frac{2K}{2K}\delta_{ij}}{2K} \tag{9.186}$$

the combination of (9.179) and (9.183) gives using the definition

$$\overline{d}_{ij} + \overline{\omega}_{ij} = \frac{\partial \overline{v}_i}{\partial x_j} , \tag{9.187}$$

the relationship

$$\frac{Db_{ij}}{Dt} = -b_{ij}\left(\frac{\mathcal{P}}{K} - \varepsilon\right) - \frac{2}{3}\overline{d}_{ij} - \left(b_{ik}\overline{d}_{kj} + \overline{d}_{ik}b_{kj} - \frac{2}{3}b_{mn}\overline{d}_{mn}\delta_{ij}\right)$$

$$+ \left(b_{ik}\overline{\omega}_{kj} - \overline{\omega}_{ik}b_{kj}\right) + \frac{\Pi_{ij}}{2K} + \frac{1}{2K}\left(\mathcal{D}_{ij} - \frac{\tau_{ij}}{K}\mathcal{D}\right) - \frac{1}{\tau}d_{ij} , \tag{9.188}$$

with $\tau = K/\varepsilon$.

To treat the pressure-strain rate correlation, we take the divergence of (9.19) that produces the pressure Poisson's equation

$$\frac{1}{\rho}\frac{\partial^2 p'}{\partial x_i^2} = -2\frac{\partial v'_i}{\partial x_j}\frac{\partial \overline{v}_j}{\partial x_i} - \left(\frac{\partial v'_i}{\partial x_j}\frac{\partial v'_j}{\partial x_i} - \overline{\frac{\partial v'_i}{\partial x_j}\frac{\partial v'_j}{\partial x_i}}\right) . \tag{9.189}$$

It is customary (cf. [24]) to decompose the turbulent pressure field p' into slow $p'^{(s)}$ and rapid $p'^{(r)}$ contributions

$$\frac{1}{\rho}\frac{\partial^2 p'^{(s)}}{\partial x_i^2} = -\left(\frac{\partial v'_i}{\partial x_j}\frac{\partial v'_j}{\partial x_i} - \overline{\frac{\partial v'_i}{\partial x_j}\frac{\partial v'_j}{\partial x_i}}\right) \tag{9.190}$$

$$\frac{1}{\rho}\frac{\partial^2 p'^{(r)}}{\partial x_i^2} = -2\frac{\partial v'_i}{\partial x_j}\frac{\partial \overline{v}_j}{\partial x_i} . \tag{9.191}$$

Equation (9.190) expresses the "slow" relaxation of the turbulence toward isotropy while (9.191) is concerned with the "rapid" response of turbulence to imposed mean velocity gradients.

The modeling of the pressure-strain rate correlation is based on the hypothesis of local homogeneity. Therefore, for the case of a one-point closure, the model is based on functionals of the Reynolds stress and the turbulent dissipation rate. We write

$$\Pi_{ij} = \varepsilon \mathcal{A}_{ij}(\boldsymbol{b}) + K \mathcal{M}_{ij}(\boldsymbol{b}) . \tag{9.192}$$

Gatski and Jongen [32] propose a nonlinear form in the anisotropy tensor b_{ij} that reads

$$\begin{aligned}
\Pi_{ij} = &-\left(C_1^0 + C_1^1\frac{\mathcal{P}}{\varepsilon}\right)\varepsilon b_{ij} + C_2 K \overline{d}_{ij} \\
&+ C_3 K \left(b_{ik}\overline{d}_{jk} + b_{jk}\overline{d}_{ik} - \frac{2}{3}b_{mn}\overline{d}_{mn}\delta_{ij}\right) \\
&- C_4 K \left(b_{ik}\overline{\omega}_{kj} - \overline{\omega}_{ik}b_{kj}\right) \\
&+ C_5 \varepsilon \left(b_{ik}b_{kj} - \frac{1}{3}b_{mn}b_{nm}\delta_{ij}\right) .
\end{aligned} \tag{9.193}$$

Substituting (9.193) in (9.188) and rewriting yields

$$\begin{aligned}
\frac{Db_{ij}}{Dt} &- \frac{1}{2K}\left(\mathcal{D}_{ij} - \frac{\tau_{ij}}{K}\mathcal{D}\right) \\
&= -\left(\frac{b_{ij}}{a_4} + a_3\left(b_{ik}\overline{d}_{kj} + \overline{d}_{ik}b_{kj} - \frac{2}{3}b_{mn}\overline{d}_{mn}\delta_{ij}\right)\right. \\
&\quad - a_2\left(b_{ik}\overline{\omega}_{kj} - \overline{\omega}_{ik}b_{kj}\right) + a_1\overline{d}_{ij} \\
&\quad \left. - \frac{1}{\tau}a_5\left(b_{ik}b_{kj} - \frac{1}{3}b_{mn}b_{nm}\delta_{ij}\right) + \frac{1}{\tau}d_{ij}\right) ,
\end{aligned} \tag{9.194}$$

with the pressure-strain rate closure coefficients

$$a_1 = \frac{1}{2}\left(\frac{4}{3} - C_2\right) , \quad a_2 = \frac{1}{2}\left(2 - C_4\right) ,$$

$$a_3 = \frac{1}{2}\left(2 - C_3\right) , \tag{9.195}$$

$$a_4 = \tau \left(\frac{C_1^0}{2} - 1 + \left(\frac{C_1^1}{2} + 1\right)\frac{\mathcal{P}}{\varepsilon}\right)^{-1} ,$$

$$a_5 = \frac{1}{2}C_5 . \tag{9.196}$$

The closure coefficients are obtained from experimental data or numerical results on benchmark problems. Following Speziale et al. [96], we have $C_1^0 = 3.4, C_1^1 = 1.8, C_2 = 0.36, C_3 = 1.25, C_4 = 0.4, C_5 = 4.2$.

9.12 Reynolds Stress Tensor Representation Using Integrity Bases

From the previous section, we know that

$$b = b\left(\overline{d}, \overline{\overline{\omega}}, \tau\right) , \tag{9.197}$$

where τ is the integral turbulence time. The tensor b must satisfy the isotropy property, namely

$$Qb\left(\overline{d}, \overline{\overline{\omega}}, \tau\right)Q^T = b\left(Q\overline{d}Q^T, Q\overline{\overline{\omega}}Q^T, \tau\right) , \tag{9.198}$$

for all orthogonal transformation matrices Q such that $QQ^T = Q^TQ = I$ and det $Q = \pm 1$, where Q^T is the transpose of Q and det denotes the determinant. By (9.198), it is required that b be invariant to the full orthogonal group that includes all reflection and rotation matrices. By the Cayley–Hamilton theorem (9.175), given an arbitrary finite set of input tensors, it is possible to construct a finite basis of invariant tensors, called an integrity basis [24]. Any invariant tensor function of these given tensors, $\overline{d}, \overline{\overline{\omega}}$, will be a linear combination of the integrity basis tensors. These integrity bases have been tabulated in chapter two of Deville-Gatski monograph [24] where a clear presentation is aimed at achieving readability.

To summarize the theoretical development that is beyond the scope of this monograph, the integrity basis for a single symmetric tensor T is given by the associated matrix invariants

$$\text{tr } T, \text{tr } T^2, \text{tr } T^3 . \tag{9.199}$$

For the case of a product of two tensors T, U the matrix products to be considered are

$$TU, TU^2, UT^2, T^2U^2, TUT^2U^2 \tag{9.200}$$

and the invariants associated with the matrix products of T and U are

$$\operatorname{tr} TU, \operatorname{tr} TU^2, \operatorname{tr} UT^2, \operatorname{tr} T^2U^2, \operatorname{tr} TUT^2U^2 . \tag{9.201}$$

Of these five invariants the first four are irreducible. A polynomial invariant is called irreducible if it cannot be expressed as a polynomial in other invariants. The fifth invariant in (9.201) can be written in terms of the irreducible invariants. As a consequence, the resulting integrity basis for symmetric second-order tensors consist of

$$\operatorname{tr} T, \operatorname{tr} T^2, \operatorname{tr} T^3, \operatorname{tr} TU, \operatorname{tr} TU^2, \operatorname{tr} UT^2, \operatorname{tr} T^2U^2 . \tag{9.202}$$

We want to develop a general representation for the anisotropy tensor for turbulent flows. Our minimal integrity basis for the tensors $\overline{d}$ and $\overline{\omega}$ is given by

$$\eta_1 = \operatorname{tr} \overline{d}^2, \quad \eta_2 = \operatorname{tr} \overline{\omega}^2, \quad \eta_3 = \overline{d}^3,$$
$$\eta_4 = \operatorname{tr} \overline{\omega}^2\overline{d}, \quad \eta_5 = \operatorname{tr} \overline{\omega}^2\overline{d}^2, \quad \eta_6 = \operatorname{tr} \overline{d}\,\overline{\omega}\,\overline{d}^2\overline{\omega}^2 . \tag{9.203}$$

Rivlin and Ericksen [80] showed that it is possible to write a linear relation between the dependent tensor b and a finite number N of other tensors $T^{(1)}, T^{(2)}, \ldots, T^{(N)}$ formed from the elements of the independent tensors $\overline{d}$ and $\overline{\omega}$

$$\alpha_0 b = \sum_{n=1}^{N} \alpha_n T^{(n)} . \tag{9.204}$$

The linear system (9.204) is solved by projecting it onto the $T^{(n)}$ basis in a way very similar to a Galerkin projection, the details of which are left for the curious and interested reader in the paper by Jongen and Gatski [40]. For a five term representation $N = 5$, the basis reduces to

$$T^{(1)} = \overline{d}, \quad T^{(2)} = \overline{d}\,\overline{\omega} - \overline{\omega}\,\overline{d}, \quad T^{(3)} = \overline{d}^2 - \frac{1}{3}(\operatorname{tr} \overline{d}^2)I$$
$$T^{(4)} = \overline{\omega}^2 - \frac{1}{3}(\operatorname{tr} \overline{\omega}^2)I, \quad T^{(5)} = \overline{\omega}\,\overline{d}^2 - \overline{d}^2\overline{\omega} . \tag{9.205}$$

We leave at this stage the detailed writing of the final form of the equations. Further considerations may be found for turbulence modeling in Deville-Gatski [24] where are tackled the closure for the dissipation rate tensor, low-Reynolds turbulence modeling and the important engineering problem related to the constraints imposed by the presence of solid boundaries.

9.13 Large Eddy Simulation

RANS models even though as sophisticated as they might be have produced in some cases dismal performances and failed to resolve properly the turbulent physical phenomena. As the advent of more powerful computers made computational fluid dynamics (CFD) a more amenable way to tackle turbulence, the large eddy simulation (LES) became the appropriate tool.

LES comes from the observation that these large structures depend strongly on the flow type under scrutiny through the geometrical configuration, the boundary conditions, etc., while the small scales are more universal and therefore simpler to model. Moreover, as we will resort to numerical computation to integrate the equations (e.g. CFD), the large scales will be resolved by the simulation inasmuch the computational mesh be fine enough, while the small structures whose characteristic size is much lower than the mesh size, will be taken into account by a sub-grid model.

We will compute the motion of the large turbulent structures and their dynamics by the transient three-dimensional simulation in the flow domain. The statistical properties of the flow will be obtained by time averaging and/or by spatial means in the homogeneous (periodic) planes or by repeating several computations. This last possibility is never carried out because of its sky-rocketing cost.

This section is only an introduction to the subject and is missing a lot of details, interesting comments and presentation of the many LES models. The interested reader is referred to the monographs of P. Sagaut [84] and L. Berselli et al. [15] for a complete LES analysis.

9.13.1 Definitions

Let us consider the function $f(\boldsymbol{x}, t)$. The filtered field $\tilde{f}$ is defined by the convolution product

$$\tilde{f}(\boldsymbol{x}, t) = \int_{-\infty}^{\infty} G(\boldsymbol{x}, \boldsymbol{x}'; \Delta_{\boldsymbol{x}}) f(\boldsymbol{x}', t) \, d^3\boldsymbol{x}' \, . \tag{9.206}$$

The filtering function G allows to determine exactly which proportion (spatially speaking) of the flow will be incorporated in the large scales. The filtering parameter $\Delta_{\boldsymbol{x}}$ is used to fix this choice. In a compact form, this relation reads

$$\tilde{f} = G \star f \, , \tag{9.207}$$

where $G\star$ represents the filtering operator. The filter function is normalized such that

$$\int_{-\infty}^{\infty} G(\boldsymbol{x}, \boldsymbol{x}'; \Delta_{\boldsymbol{x}}) \, d^3\boldsymbol{x}' = 1, \quad \forall \boldsymbol{x} \, . \tag{9.208}$$

The residual field f' is the complement of the filtered function

$$f(\boldsymbol{x}, t) = \tilde{f}(\boldsymbol{x}, t) + f'(\boldsymbol{x}, t) . \tag{9.209}$$

The filtered field unlike what occurs in the Reynolds decomposition, **does not vanish**. Indeed, we can verify that

$$\tilde{\tilde{f}} \neq \tilde{f}, \quad \tilde{f}' \neq 0 . \tag{9.210}$$

Filtering (9.209), one obtains the residual filtered field

$$\tilde{f}' = \tilde{f} - \tilde{\tilde{f}} . \tag{9.211}$$

In the particular case of homogeneous turbulence, the filter has the simpler form $G(\boldsymbol{x} - \boldsymbol{x}'; \Delta_{\boldsymbol{x}})$. Consequently, the equation

$$\tilde{f}(\boldsymbol{x}, t) = \int G(\boldsymbol{x} - \boldsymbol{x}'; \Delta_{\boldsymbol{x}}) f(\boldsymbol{x}', t) \, d^3\boldsymbol{x}' \tag{9.212}$$

is Fourier transformed into

$$\hat{\tilde{f}}(\boldsymbol{k}, t) = \hat{G}(k; \Delta_{\boldsymbol{x}}) \, \hat{f}(\boldsymbol{k}, t) . \tag{9.213}$$

Here, we observe that G depends only on the norm k of the wavevector $\boldsymbol{k}$. For the Fourier case, various filters have been elaborated. The sharp cut-off filter corresponds to set all high frequency modes to zero beyond the cut-off frequency k_c in spectral space. This practice produces a clear separation between small and large scales

$$\hat{G} = \begin{cases} 1 \text{ if } \mid k_i - k_i' \mid \leq k_c, \\ 0 \text{ otherwise} . \end{cases} \tag{9.214}$$

However, the filtered signal obtained by inverse Fourier transform in the physical space presents a Gibbs phenomenon, which complicates the flow interpretation. A more even filter is defined with the Gaussian filter

$$G(\boldsymbol{x} - \boldsymbol{x}', \Delta_{\boldsymbol{x}}) = C \exp^{-6(x_i - x_i')^2/\Delta^2} , \tag{9.215}$$

where the constant C depends on the normalisation. The Fourier transform of the Gaussian filter is also Gaussian.

9.13.2 LES Equations

The velocity is decomposed as

$$\boldsymbol{v} = \tilde{\boldsymbol{v}} + \boldsymbol{v}' . \tag{9.216}$$

The filtered incompressibility equation yields

$$\nabla \cdot \tilde{v} = 0 \,, \tag{9.217}$$

so that by subtracting (9.217) from the continuity equation, one obtains

$$\nabla \cdot v' = 0 \,. \tag{9.218}$$

The resolved and residual velocity fields are incompressible. Filtering the Navier–Stokes equations, one gets

$$\frac{\partial \tilde{v}}{\partial t} + \nabla \cdot (\tilde{v}\, \tilde{v}) \;=\; -\nabla \tilde{p} + \nu \triangle \tilde{v} - \nabla \cdot \boldsymbol{\tau}, \tag{9.219}$$

$$\operatorname{div} \tilde{v} = 0. \tag{9.220}$$

The sub-grid stress (SGS) tensor $\boldsymbol{\tau}$ takes into account the small scales effects on the dynamics of the resolved scales and is given by

$$\boldsymbol{\tau} = \widetilde{vv} - \tilde{v}\, \tilde{v}. \tag{9.221}$$

With the decomposition (9.216), the SGS tensor may be redefined as

$$\boldsymbol{\tau} = \mathcal{L} + \mathcal{C} + \mathcal{R} \,, \tag{9.222}$$

where

$$\begin{aligned}
\mathcal{L} &= \widetilde{\tilde{v}\, \tilde{v}} - \tilde{\tilde{v}}\, \tilde{\tilde{v}} \,, \\
\mathcal{C} &= (\widetilde{\tilde{v}\, v' + v'\tilde{v}}) - (\tilde{\tilde{v}}\, \tilde{v}' + \tilde{v}'\, \tilde{\tilde{v}}) \,, \\
\mathcal{R} &= \widetilde{v'v'} - \tilde{v}'\, \tilde{v}' \,,
\end{aligned} \tag{9.223}$$

are the Leonard stress, $\mathcal{L}$, and the SGS cross terms, $\mathcal{C}$, together with the Reynolds stress, $\mathcal{R}$, respectively. The Leonard term can be computed by the resolved quantities. The cross tensor $\mathcal{C}$ represents the interactions between resolved and unresolved scales. The turbulent stress tensor $\mathcal{R}$ represents the interaction between unresolved small scales.

9.13.3 The Smagorinsky Model

The Smagorinsky SGS model (SM) [92] utilises the concept of turbulent viscosity ν_T and is given by the relation

$$\boldsymbol{\tau} - \frac{1}{3} tr(\boldsymbol{\tau})\, \mathbf{I} = -2\nu_T \tilde{\boldsymbol{S}} = -2C_S \tilde{\Delta}^2 (\mathrm{II}_{\tilde{\boldsymbol{S}}})^{1/2} \tilde{\boldsymbol{S}} = -2C_S \boldsymbol{b}, \qquad (9.224)$$

where $\tilde{\boldsymbol{S}}$ is the filtered strain rate tensor

$$\tilde{\boldsymbol{S}} = \frac{1}{2}(\widetilde{\nabla \boldsymbol{v}} + \widetilde{(\nabla \boldsymbol{v})}^T), \qquad (9.225)$$

and the tensor $\boldsymbol{b}$ is defined as

$$\boldsymbol{b} = \tilde{\Delta}^2 (\mathrm{II}_{\tilde{\boldsymbol{S}}})^{1/2} \tilde{\boldsymbol{S}}\,. \qquad (9.226)$$

The constant C_S is the Smagorinsky constant such that $C_S \approx 0.18$, $\tilde{\Delta}$ the filter size and $\mathrm{II}_{\tilde{\boldsymbol{S}}}$ the second invariant of $\tilde{\boldsymbol{S}}$. The symbol tr denotes the trace of the tensor. The SM presents several flaws. The most severe one consists in the C_S constant value during the computation and this defect produces too much dissipation. Furthermore, the SM does not allow backscatter that transfers kinetic energy from small to large scales in the opposite direction of Richardson cascade. Finally, in the a priori tests where the correlation between the modeled tensor and the exact SGS tensor (9.221) is evaluated, one obtains poor quality results.

9.13.4 The Dynamic Model

The dynamic model (DM) proposed by Germano et al. [35] circumvents the difficulty of the constant C_S by letting it depend on space and time. We thus have a dynamic parameter $C_d = C_d(\boldsymbol{x}, t)$. Let us introduce the length-scale of a test-filter $\hat{\Delta}$ that is larger than the mesh length-scale $\tilde{\Delta}$ (e.g. $\hat{\Delta} = 2\tilde{\Delta}$). Using the information provided by both filters and assuming that in the inertial part of the turbulent energy spectrum, the statistical self-similarity applies, we can better determine the characteristics of the SGS tensor. The scale-similarity hypothesis assumes that the behavior of the smallest resolved scales is similar to the subgrid unresolved scales being modeled. With the test filter, the previous LES equations (9.219) lead to a relation implying the sub-tests scales stresses

$$\boldsymbol{T} = \widehat{\widetilde{\boldsymbol{v}}\widetilde{\boldsymbol{v}}} - \hat{\tilde{\boldsymbol{v}}}\,\hat{\tilde{\boldsymbol{v}}}\,. \qquad (9.227)$$

One introduces Germano's identity to obtain the relation between $\boldsymbol{T}$ and the SGS filtered tensor $\hat{\boldsymbol{\tau}}$ such that

$$\mathcal{G} = \boldsymbol{T} - \hat{\boldsymbol{\tau}} = \widehat{\tilde{\mathbf{v}}\,\tilde{\mathbf{v}}} - \hat{\tilde{\mathbf{v}}}\,\hat{\tilde{\mathbf{v}}}. \qquad (9.228)$$

Applying the turbulent viscosity model to $\boldsymbol{T}$ and using the self-similarity hypothesis for the C_d constant, one obtains

$$\boldsymbol{T} - \frac{1}{3}tr(\boldsymbol{T})\,\mathbf{I} = -2C_d\hat{\Delta}^2(\mathrm{II}_{\hat{\mathbf{S}}})^{1/2}\hat{\hat{\mathbf{S}}} := -2C_d\boldsymbol{a}. \tag{9.229}$$

Inserting (9.224) and (9.229) in the deviatoric part of $\mathcal{G}$, one has

$$\mathcal{G} - \frac{1}{3}tr(\mathcal{G})\mathbf{I} = 2(\widehat{C_d\boldsymbol{b}} - C_d\boldsymbol{a}). \tag{9.230}$$

Supposing that C_d does not vary too much in space, we set $\hat{C}_d \approx C_d$ and then we deduce from a least square minimisation of the error linked to (9.230) (cf. [51] for details) that

$$C_d = -\frac{1}{2}\frac{\mathcal{M}:\mathcal{G}}{\mathcal{M}:\mathcal{M}}, \tag{9.231}$$

where

$$\mathcal{M} = \boldsymbol{a} - \hat{\boldsymbol{b}} \tag{9.232}$$

and the notation : designates the inner tensorial product (double contraction).

In the case where the flow has no homogeneous direction, the previous hypothesis about the slow spatial variation of C_d and its elimination of the filtering operation are no longer valid. To avoid this difficulty, we follow the procedure proposed by Piomelli and Liu [72]. Taking the scalar product of Eq. (9.230) with $\boldsymbol{a}$, one obtains the relation

$$C_d = -\frac{1}{2}\frac{(\mathcal{L} - \frac{1}{3}tr(\mathcal{L})\mathbf{I} - 2\widehat{C^*\boldsymbol{b}}):\boldsymbol{a}}{\boldsymbol{a}:\boldsymbol{a}}, \tag{9.233}$$

where the known quantity $C^* = C_d^{n-1}$, i.e. the C_d value at the former time level in the CFD time integration scheme.

9.13.5 The Dynamic Mixed Model

The dynamic mixed model [126] introduced to simulate cavity flows is a blending of the mixed model of Bardina et al. [8] and of the previous dynamic model. Note that the mixed model is not a model based on the turbulent viscosity. On the contrary it belongs to the class of structural models [84] and rests upon the similarity principle of scales. It hardly produces dissipation and for that reason we must use it with the dynamic model. We decompose the velocity field in a resolved field and a sub-grid field as done in Eq. (9.216) and we redefine the stress as Germano [34] proposed in Eqs. (9.221)–(9.223). The Leonard term computed by the resolved quantities corresponds essentially to the mixed models. The other two terms are the non resolved residual stresses and they are treated via the Smagorinsky model. The dynamic procedure is applied to the C constant in order to obtain a dynamic coefficient. Let us introduce

a test filter denoted now by a hat $\hat{}$. By application of the test filter to (9.219), one generates the sub-tests scales stress

$$T = \widehat{\widetilde{vv}} - \hat{\tilde{v}}\,\hat{\tilde{v}} = L^t + C^t + R^t, \tag{9.234}$$

with

$$
\begin{aligned}
L^t &= \widehat{\widehat{\tilde{v}}\,\tilde{v}} - \hat{\tilde{v}}\,\hat{\tilde{v}} \\
C^t &= (\widetilde{\tilde{v}\,v' + v'\tilde{v}}) - (\hat{\tilde{v}}\,\hat{v}' + \hat{v}'\,\hat{\tilde{v}}), \\
R^t &= \widehat{\widehat{v'v'}} - \hat{v}'\,\hat{v}'.
\end{aligned}
\tag{9.235}
$$

The deviatoric turbulent stress tensors associated with the sub-grid and sub-tests filters are expressed as follows

$$
\begin{aligned}
\boldsymbol{\tau} - \frac{1}{3}tr(\boldsymbol{\tau})\,\mathbf{I} &= -2C_d \tilde{\Delta}^2 (\mathrm{II}_{\tilde{\mathbf{S}}})^{1/2}\tilde{\mathbf{S}} + \mathcal{L} - \frac{1}{3}tr(\mathcal{L})\,\mathbf{I} \\
&= -2C_d \boldsymbol{b} + \mathcal{L} - \frac{1}{3}tr(\mathcal{L})\,\mathbf{I}, \tag{9.236} \\
T - \frac{1}{3}tr(T)\,\mathbf{I} &= -2C_d \hat{\tilde{\Delta}}^2 (\mathrm{II}_{\hat{\tilde{\mathbf{S}}}})^{1/2}\hat{\tilde{\mathbf{S}}} + L^t - \frac{1}{3}tr(L^t)\,\mathbf{I} \\
&= -2C_d \boldsymbol{a} + L^t - \frac{1}{3}tr(L^t)\,\mathbf{I}. \tag{9.237}
\end{aligned}
$$

Substituting Eqs. (9.236) and (9.237) in Germano's identity (9.228) and introducing tensor $\mathcal{H}$

$$\mathcal{H} = \widehat{\widehat{\tilde{v}}\,\tilde{v}} - \hat{\tilde{v}}\,\hat{\tilde{v}} \tag{9.238}$$

one evaluates the C constant following the same steps as for the dynamic model

$$C = -\frac{1}{2}\frac{((\mathcal{G} - \mathcal{H}) - 2\widehat{C^*\boldsymbol{b}}) : \boldsymbol{a}}{\boldsymbol{a} : \boldsymbol{a}}. \tag{9.239}$$

9.13.6 The Approximate Deconvolution Method

The approximate deconvolution method (ADM) [98, 99] extracts the information of the resolved scales in order to deduce from them the behavior of the sub-grid scales. The founding hypothesis leading to ADM consists in the existence of G^{-1} that can be computed by a finite series in $\tilde{v}$. As $G = I - (I - G)$, the inverse of G may be written as a non convergent series

$$G^{-1} = \sum_{n=0}^{\infty} (I - G)^n \,. \tag{9.240}$$

Van Cittert [113] proposed to approximate G^{-1} by a finite series such as

$$G_a^{-1} := Q_M = \sum_{n=0}^{M} (I_d - G)^n \,, \tag{9.241}$$

where I_d is the identity operator.

The ADM approach constructs an approximation of the velocity field $\boldsymbol{v}^*$ that must be used in the non-linear term

$$\boldsymbol{v}^* = Q_M \star (G \star \boldsymbol{v}). \tag{9.242}$$

The deconvolutions to order three and five yield

$$\boldsymbol{v}^* = Q_3 \star \tilde{\boldsymbol{v}} = 4(\tilde{\boldsymbol{v}}^{(1)} + \tilde{\boldsymbol{v}}^{(3)}) - 6\tilde{\boldsymbol{v}}^{(2)} - \tilde{\boldsymbol{v}}^{(4)}, \tag{9.243}$$

$$\boldsymbol{v}^* = Q_5 \star \tilde{\boldsymbol{v}} = 6(\tilde{\boldsymbol{v}}^{(1)} + \tilde{\boldsymbol{v}}^{(5)}) - 15(\tilde{\boldsymbol{v}}^{(2)} + \tilde{\boldsymbol{v}}^{(4)}) + 20\tilde{\boldsymbol{v}}^{(3)} - \tilde{\boldsymbol{v}}^{(6)}, \tag{9.244}$$

with the notation $\tilde{\boldsymbol{v}}^{(k)}$ indicating that the velocity field is filtered k times.

We then solve the set of equations

$$\frac{\partial \tilde{\boldsymbol{v}}}{\partial t} + (\widetilde{\nabla \cdot \boldsymbol{v}^* \boldsymbol{v}^*}) = -\nabla \tilde{p} + \nu \Delta \tilde{\boldsymbol{v}}, \tag{9.245}$$

$$\mathrm{div}\,\tilde{\boldsymbol{v}} = 0. \tag{9.246}$$

9.14 Concluding Remarks

At the end of this chapter the reader may feel overwhelmed, lonely and trapped in a chaotic ocean of equations, models and choices that are not obvious. Fortunately enough, some researchers felt the same and wrote review articles like the paper by Argyropoulos and Markatos [4] to delineate the pros and cons of each approach versus the target to be reached within a given time frame.

It is of course a complete different situation to solve an engineering problem using a RANS model because it should be done within minutes rather than getting a nice simulation by an LES approach that requires weeks or months of computing time on a large parallel machine. Therefore the choice of the turbulence model depends on many parameters: the time allotted to solving the problem, the computer available, the accuracy demanded (a few percents like in most engineering design or more

precision). Is computing a trend instead a full solution sufficient if one changes only one data, do we need a physically meaning solution?, etc.

Whatever complicated the situation is, there remains still hope for improvement and better comprehension of turbulence. I will finish by quoting Sébastien Galtier [31] in his introduction (my own translation) "A detailed analytical understanding of turbulence remains limited because of the difficulty intrinsic to non-linear physics. Therefore one often reads that turbulence is one of the last major non solved problems of the classical physics. This long conveyed affirmation that can be found in the book of Feynman [29] does no longer correspond to the modern view. Indeed, even though turbulence remains a very active research subject, we have today availability to many theoretical, experimental and observational results which allow us to know in detail the physics of turbulence".

Exercises

9.1 Prove relation (9.53)

9.2 Show that the two-point velocity correlation tensor (9.60) is symmetric.

9.3 Demonstrate Eqs. (9.243) and (9.244).